NAVAL POSTGRADUATE SCHOOL
Monterey, California

THESIS

BARREL WEAR REDUCTION IN RAIL GUNS: AN INVESTIGATION OF SILVER PASTE LIQUID-METAL INTERFACE

by

Michael Willet Smith Jr.

December 2002

Thesis Advisor:	William B. Maier II
Thesis Co-Advisor:	Donald Snyder
Second Reader:	Richard Harkins

THIS PAGE INTENTIONALLY LEFT BLANK

REPORT DOCUMENTATION PAGE			Form Approved OMB No. 0704-0188

1. AGENCY USE ONLY *(Leave blank)*	2. REPORT DATE December 2002	3. REPORT TYPE AND DATES COVERED Master's Thesis

4. TITLE AND SUBTITLE: Barrel Wear Reduction in Rail Guns: An Investigation of Silver Paste Liquid-Metal Interface	5. FUNDING NUMBERS
6. AUTHOR(S) Michael Willet Smith Jr.	
7. PERFORMING ORGANIZATION NAME(S) AND ADDRESS(ES) Naval Postgraduate School Monterey, CA 93943-5000	8. PERFORMING ORGANIZATION REPORT NUMBER
9. SPONSORING /MONITORING AGENCY NAME(S) AND ADDRESS(ES) N/A	10. SPONSORING/MONITORING AGENCY REPORT NUMBER

11. SUPPLEMENTARY NOTES The views expressed in this thesis are those of the author and do not reflect the official policy or position of the Department of Defense or the U.S. Government.

12a. DISTRIBUTION / AVAILABILITY STATEMENT Approved for public release; distribution is unlmited	12b. DISTRIBUTION CODE

13. ABSTRACT ***(maximum 200 words)***

This thesis tests the effects a commercial silver paste has on the damage at the projectile-rail interface of a 4" long rail gun test section. Projectiles (0.635 x 0.635 x 0.953 cm) were pushed through the rail test section at 34 $\pm$ 19 m/s, while average current densities of 18-32 kA/cm^2 was passed through the projectile – rail interface material. The specific objective is to examine rail and projectile damage at current densities near or above those ($\approx$ 25kA/cm^2) anticipated for a naval rail gun. Voltages across the rails were monitored and changes in conductivity when solid electrical contact was broken were observed. Silver deposits were observed on the rails from the paste at a peak current of 13.3 kA, while no damage was seen on the rails until a peak current of 17.2 kA was reached, which corresponds to average current densities of 22 kA/cm^2 and 28.5 kA/cm^2, respectively.

14. SUBJECT TERMS Rail Gun, Railgun, Sliding Contact, Electrical Contact, Conductive Interface, Silver Paste, Rail Erosion, Projectile Diagnostics	15. NUMBER OF PAGES 63
	16. PRICE CODE

17. SECURITY CLASSIFICATION OF REPORT	18. SECURITY CLASSIFICATION OF THIS PAGE	19. SECURITY CLASSIFICATION OF ABSTRACT	20. LIMITATION OF ABSTRACT
Unclassified	Unclassified	Unclassified	UL

NSN 7540-01-280-5500 Standard Form 298 (Rev. 2-89)
Prescribed by ANSI Std. 239-18

THIS PAGE INTENTIONALLY LEFT BLANK

Approved for public release; distribution is unlimited

BARREL WEAR REDUCTION IN RAIL GUNS: AN INVESTIGATION OF SILVER PASTE LIQUID-METAL INTERFACE

Michael Willet Smith Jr.
Lieutenant, United States Navy
B.S., Southern University, 1998

Submitted in partial fulfillment of the
requirements for the degree of

MASTER OF SCIENCE IN APPLIED PHYSICS

from the

NAVAL POSTGRADUATE SCHOOL
December 2002

Author: Michael Willet Smith, Jr.

Approved by: William B. Maier II
Thesis Advisor

Donald Snyder
Thesis Co-Advisor

Richard Harkins
Second Reader

William B. Maier II
Chairman, Department of Physics

THIS PAGE INTENTIONALLY LEFT BLANK

ABSTRACT

This thesis tests the effects a commercial silver paste has on the damage at the projectile-rail interface of a 4" long rail gun test section. Projectiles (0.635 x 0.635 x 0.953 cm) were pushed through the rail test section at 34 $\pm$19 m/s, while average current densities of 18 - 32 kA/cm^2 was passed through the projectile – rail interface material. The specific objective is to examine rail and projectile damage at current densities near or above those ($\approx$25kA/cm^2) anticipated for a naval rail gun. Voltages across the rails were monitored and changes in conductivity when solid electrical contact was broken were observed. Silver deposits were observed on the rails from the paste at a peak current of 13.3 kA, while no damage was seen on the rails until a peak current of 17.2 kA was reached, which corresponds to average current densities of 22 kA/cm^2 and 28.5 kA/cm^2, respectively.

THIS PAGE INTENTIONALLY LEFT BLANK

TABLE OF CONTENTS

I. INTRODUCTION 1
A. PURPOSE 1
B. HISTORY 1
1. Why is the Rail Gun the Weapon of Choice for the U.S. Navy? 1
2. Possible Considerations 2
C. RAIL GUN THEORY 3
D. BARREL WEAR 5
E. MOTIVATION FOR THESIS 7

II. THE EXPERIMENTAL METHOD 9
A. EQUIPMENT USED 9
B. POWER SUPPLY 9
C. ADDED INDUCTANCE 11
D. CURRENT DENSITY 13
E. PARTS 15
1. Accelerator 15
2. Pusher Housing 16
3. Pusher Assembly 17
F. TRIGGER BOX AND DELAY GENERATOR 18
G. DIFFERENTIAL AMPLIFIER 19
H. VARIABLE GRAPHITE RESISTOR 20
I. VELOCITY MEASUREMENTS WITH THE DIFFERENTIAL AMPLIFIER 21

III. TEST RESULTS 23
A. PROJECTILE VELOCITY RESULTS 23
B. UNIFORM CONTACT BETWEEN PROJECTILE AND RAILS 29
C. NON-UNIFORM CONTACT BETWEEN PROJECTILE AND RAILS. 30
D. THE SILVER PASTE AS AN INTERFACE MATERIAL 32

IV. CONCLUSION 41

V. FUTURE WORK 43

LIST OF REFERENCES 45

INITIAL DISTRIBUTION LIST 47

THIS PAGE INTENTIONALLY LEFT BLANK

LIST OF FIGURES

Figure 1. Illustration of the Lorentz Force 4
Figure 2. Generated Magnetic Field 4
Figure 3. Rail Erosion due to 5.5 kV Discharge from Power Supply Capacitors 6
Figure 4. Schematic of the Major Components of the Power Supply 10
Figure 5. Overhead View of Power Supply 11
Figure 6. Characteristic Exponential Decay Curve of Current vs. Time, L = 2.5, C = 1660 μH , R = 9 $m\Omega$, Voltage across the Capacitors, V_c = 2.25 kV. 11
Figure 7. Graphic Representation of Current Density 13
Figure 8. Current pulse. Ordinate scale is 1 V per division. Abscissa scale is 1 ms per division. 14
Figure 9. Computer Generated Graphical Representation of the Accelerator 15
Figure 10. Pusher Housing with Dimensions 16
Figure 11. Pusher Assembly with Aluminum and Neoprene disks 17
Figure 12. Trigger Box with Fiber Optic Cables 18
Figure 13. Model DG535 Four Channel Digital Delay/Pulse Generator 19
Figure 14. Lecroy DA1822A Differential Amplifier 19
Figure 15. Laser, Photodetector, and Variable Graphite Resistor 20
Figure 16. Laser Setup of the Rail Gun Test Platform 22
Figure 17. Delta Time at 3 kV Capacitor Charge. Ordinate scale is as indicated by the color associated with each waveform. Abscissa scale is 2 ms per division. 24
Figure 18. Delta Time at 3.6 kV Capacitor Charge. Ordinate scale is as indicated by the color associated with each waveform. Abscissa scale is 2 ms per division. 25
Figure 19. Delta Time at 3.8 kV Capacitor Charge. Ordinate scale is as indicated by the color associated with each waveform. Abscissa scale is 2 ms per division. 26
Figure 20. Plot of Average Velocity vs. Capacitor Charge Voltage 28
Figure 21. Expanded View of Rail Gun Test Platform 29
Figure 22. Uniform Contact Between Projectile and Rails. Peak Current = 19.3 kA, J = 32 kA/cm^2 30
Figure 23. Non-Uniform Contact Between Projectile and Rails. Peak Current = 18.2 kA, J = 30.2 kA/cm^2 31
Figure 24. Plot of Current Density J (A/cm^2) vs. Capacitor Voltage 32
Figure 25. New Rail Prior to First Use 33
Figure 26. New Rail with Silver Paste Applied 34
Figure 27. Typical Appearance of Rails with Silver Paste Applied After a Shot. The projectile is also shown. Peak Current = 13.3 kA, J = 22 kA/cm^2. 35

Figure 28. Results After 2.8 kV Shot with Silver Paste Removed. Peak Current = 13.3 kA, J = 22 kA/cm^2. An indication of silver deposit can be seen on the right-hand rail. 35
Figure 29. Results After 3.0 kV Shot with Silver Paste Removed. Peak Current = 13.8 kA, J = 22.8 kA/cm^2 36
Figure 30. Results After 3.3 kV Shot with Silver Paste Removed. Peak Current = 15.5 kA, J = 25.7 kA/cm^2 37
Figure 31. Results After 3.6 kV Shot with Silver Paste Removed. Peak Current = 17.2 kA, J = 28.5 kA/cm^2 37
Figure 32. Rails Coated with Silver Paste at 3.8 kV. Peak Current = 18.2 kA, J = 30.2 kA/cm^2 38
Figure 33. Results After 3.8 kV Shot with Silver Paste Removed. Peak Current = 18.2 kA, J = 30.2 kA/cm^2 39

LIST OF TABLES

Table 1. Guide for a Fleet Rail Gun 2
Table 2. Data Table for Velocity. 27

THIS PAGE INTENTIONALLY LEFT BLANK

ACKNOWLEDGMENTS

My thesis would not have been possible without the devotion and dedication of two key individuals, Don Snyder, and Dianne Positeri from Polcraft Inc. Don was always willing to provide any help whenever possible while dealing with a myriad of other tasks. His commitment to excellence helped me develop a greater understanding, respect, and admiration for the power of experimentation and what can be gained from the successes and failures of the process as a whole. Dianne was my primary point of contact on the fabrication of parts while providing an extremely timely turn around and delivery enabling the work on my thesis to progress without any delays due to waiting on parts or material. They were always willing to go far and beyond my expectations.

I owe a special thanks and debt of gratitude to my thesis advisor, Bill Maier, for introducing me to his vision of the rail gun as a possible Naval weapon of the future, his guidance throughout my research process, and always providing the answers to a lot of pertinent questions. Throughout my thesis research, he continually brought out the best in me. Thank you to Richard Harkins, my second reader, for helping me with the editing and review process, and to George Jaksha for the fabrication of parts on short notice.

In closing, many thanks to my wife and kids for their patience, and understanding. Their support of my education while at this institution has enabled me to exceed my limitations and helped ensure my completion of the mission.

THIS PAGE INTENTIONALLY LEFT BLANK

I. INTRODUCTION

A. PURPOSE

This thesis tests the effects a commercial silver paste has on the damage at the projectile-rail interface of a 4" long rail gun test section. Projectiles (0.635 x 0.635 x 0.953 cm) were pushed through the rail test section at 34 $\pm$ 19 m/s, while currents of 11.2 – 19.3 kA were passed through the cm^2 contact region, where current distribution was not entirely uniform. The specific objective is to examine rail and projectile damage at current densities near or above those ($\approx$ 25kA/cm^2) anticipated for a naval rail gun. Voltages across the rails were monitored and changes in conductivity when solid electrical contact was broken were observed. Silver deposits were observed on the rails from the paste at a peak current of 13.3 kA, while no damage was seen on the rails until a current of 17.2 kA was reached, which corresponds to average current densities of 22 kA/cm^2 and 28.5 kA/cm^2, respectively.

B. HISTORY

The use of a rail gun for the U.S. Navy has been considered for some time, but even more so now with the advent of the all-electric ship. There are still several factors that hinder its adoption as a viable weapon for naval surface ships. One important requirement for the implementation of a naval rail gun would be a firing rate or at least 6 rounds per minute with a barrel life of approximately 3000 rounds. At this point in time, this operation is not feasible because of rail erosion caused at the projectile rail interface.

1. Why is the Rail Gun the Weapon of Choice for the U.S. Navy?

The Navy needs a weapon that can support all warfare areas and that also provides time critical targeting. The rail gun can provide a stand-off distance of 250-300 nautical mile(s) (nm) from ashore ASM (Anti-Ship Missile) threats,

which is far greater than the 13 nm provided by current gun-based ordinance, and capable of handling 100% of the Tomahawk Land Attack Missile (TLAM) engagement plans executed in Operation Allied Force, all of which were within 200 nm of the coastline. With the increased gun range, the littoral coverage area is increased allowing for greater ship mission flexibility, while increasing the area of coverage by more than 25 times that provided by the 5"/54 NSFS (Naval Surface Fire Support) weapon employed on naval ships today [1,5].

Rail gun projectiles are expected to be one-quarter the volume, and one-sixth the weight of the standard 5" rounds, while also capable of being placed on target at a velocity of 1.5 km/s, with approximately 17MJ of kinetic energy. The rail gun performance exceeds that of the 5" gun in many aspects, such as range, velocity, and kinetic energy on target. It eliminates the need for propellant charge, reduces blast over-pressure and noise, while at the same time increasing the projectile storage volume [1,5].

2. Possible Considerations

The table below from Bill Culpeper's thesis provides a guide for the possible specifications that could be expected for a fleet rail gun to be incorporated into the Navy. The parameters listed below can be used as a guideline to ensure any institutions or organizations involved in rail gun experiments can start from a common reference point [1,5].

Table 1. Guide for a Fleet Rail Gun

Flight Mass	**15 kg**
Launch Body	**20 kg**
Launch Velocity	**2.5 km/s**
Muzzle Energy	**63 MJ**
Launch Acceleration	**30-45 Kgees**
Breech Energy	**150 MJ**
Barrel Length	**10 Meters**
Rounds Per Minute	**6-10 RPM**

It should be noted that the 5 kg difference between the flight mass and launch body as seen in Table 1 above is due to the fact that the nominal projectile is considered to be a thin aerodynamic sabot round, where the thrust-transmitting carrier is discarded from the round upon ejection from the barrel.

C. RAIL GUN THEORY

To understand the importance of this thesis, it is important to understand the theory behind the rail gun itself. Current is passed down the rails the same as in an electric circuit; however, the load resistor for the typical circuit is the sliding contact of the projectile. The current traveling in opposite directions then create counter-rotating magnetic fields, which collapse upon themselves to create a force that causes the projectile to exit the rails, called the Lorentz Force. An equation of the Lorenz Force can be seen below:

$$\overrightarrow{dF} = I(\overrightarrow{dl} x \overrightarrow{B}) \tag{1.1}$$

The following terms from the above equations are defined as follows:

$\overrightarrow{dl}$ = an element of length along the current path through the projectile

$\overrightarrow{dF}$ = an element of length of force acting on the projectile

I = the current passing through the projectile

B = the generated magnetic field

In Figure 1 below a graphic representation of the Lorentz Force can be seen:

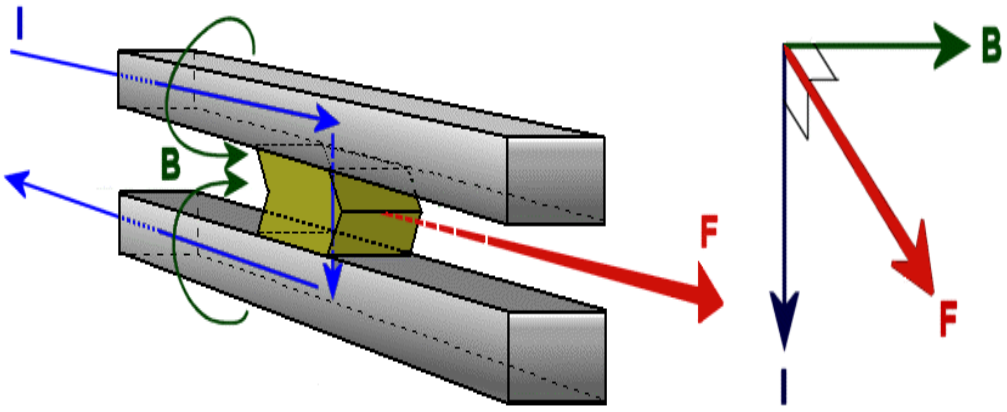

Figure 1. Illustration of the Lorentz Force

A simplified estimate of the force on the projectile can be found as follows: The rails are assumed to be a semi-infinitely long straight wire, in which case the Biot-Savart law can be used to express the generated magnetic field as seen below:

$$\vec{B} = \frac{\mu_o I}{4p\, r} \tag{1.2}$$

The following terms from the above equations are defined as follows:

μ_o = the permeability of free space

r = the radial distance from the center of the wire

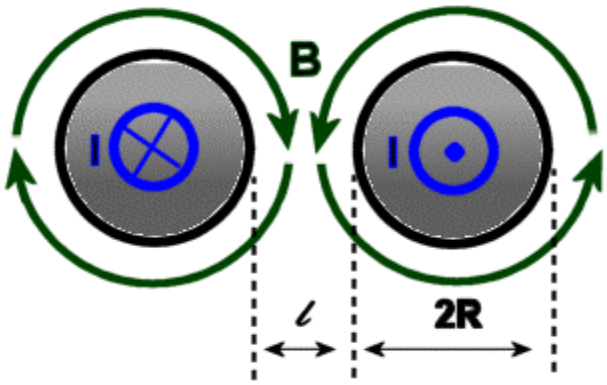

Figure 2. Generated Magnetic Field

Using equation 1.2 to estimate the magnetic field between the rails, both equations can be simplified by substituting Equation 1.2 into Equation 1.1 and then integrating to yield the following:

$$F = \frac{\mu_o I^2}{4p} \int_R^{R+1} \left(\frac{1}{x} + \frac{1}{2R + l - x} \right) dx \tag{1.3}$$

Or as follows,

$$F = \frac{\mu_o I^2}{4p} \ln \left\{ \frac{(R+l)^2}{R^2} \right\} \tag{1.4}$$

The inductance gradient, L', is defined as the change in inductance per unit length in a specified direction, and is expressed in units of (H/m) Henries per meter. Solving for the inductance gradient yields the following:

$$L' = \frac{\mu_o}{2p} \ln \left\{ \frac{(R+l)^2}{R^2} \right\} \tag{1.5}$$

*Note: The inductance gradient is dependent only on the geometrical configuration of the rail gun; therefore this is only an approximation.

Substituting Equation 1.5 into Equation 1.4 and then simplifying, the force can be expressed as seen below:

$$F = \frac{1}{2} L' I^2 \tag{1.6}$$

Although this estimate gives a rough approximation for L', Equation 1.6 represents the electromagnetic force on the projectile [1,6].

D. BARREL WEAR

Barrel wear occurs in excess of that normally arising from friction and stresses associated with magnetic fields. As the projectile slides along the bore of the rail gun, electrical heating and arcing cause damage to the projectile-rail

interface. Before a Naval rail gun can be considered as a weapon of the future, the damage sustained during firing must be minimized to increase the life of the barrel.

The factors that must be discussed when dealing with barrel wear or erosion can be classified into three categories: deposition, gouging, and arcing, sometimes associated with transition [1,2] and are defined as follows:

Depostion – the peeling off and spreading of the outer layers of the projectile along the bore.

Gouging – the removal of pieces of the rails caused by the passing projectile.

Transition – the damage inflicted by arcing upon both rails and the projectile when electrical contact cannot be maintained.

Figure 3. Rail Erosion due to 5.5 kV Discharge from Power Supply Capacitors

As discussed in Culpeper's thesis, Figure 3 provides an excellent graphic representation of the effects that high currents (60 kA) have on rail erosion when passed through a 0.635 x 0.635 x 0.953 cm projectile placed between 4-in copper tungsten rails [1].

E. MOTIVATION FOR THESIS

The rail gun is a weapon that needs to be introduced to the Navy's fleet as soon as possible due to the many advantages that it has over the current weapon system, rail guns would significantly expand the operational arena of the Battlegroup. This thesis continues in the footsteps of several other Naval Postgraduate School graduates and expands on the level of knowledge required to make the conceptual rail gun into an actual weapon of the future, possibly implemented as early as 2010. While Culpeper's thesis introduced the concept of using a silver paste as a conducting interface between the projectile and the rails, this thesis set out to find the limitations and possible characteristics of silver paste use, improve electrical contact, and thus reduce barrel heating and arcing. Minimizing the wear on the barrel does not solve all of the problems anticipated with a Naval rail gun, but it does provide valuable information in finding the probable solution required for rail gun employment.

THIS PAGE INTENTIONALLY LEFT BLANK

II. THE EXPERIMENTAL METHOD

A. EQUIPMENT USED

The test platform used in this thesis was a 4-inch gun first used by Donald Gillich, specifically designed for his thesis [7]. Many adaptations have been made on this platform and include the replacing of the phenolic spacer between the two rails used in Gillich's thesis with a more rigid 0.25-inch ceramic spacer and the use of varying shims done by Mark Adamy [2] to improve the alignment between the rails in order to provide an equal rail spacing throughout the duration of the projectile's path [1]. Adamy also improved the flexibility of the platform by adding a mechanical accelerator to test interface performance for moving projectiles at arbitrary currents. The accelerator was used in conjunction with a pusher assembly and pusher housing to transfer the momentum from the accelerator to the projectile through a non-conducting pusher placed between the rails and in direct contact with the projectile. In this way, the projectile starts moving before the power supply capacitors discharge into the rails [1].

Adamy's also introduced two separate grooved 4-inch copper tungsten rails patterns but only the groove pattern with the smaller spacing was used for this thesis. The dimensions of the projectile used for this platform are 0.25-in long, and 0.375-in wide, corresponding to 0.0938 square inches (0.604 cm^2) of surface area in direct contact with each rail [1].

Throughout the experiments conducted in this thesis, the silver paste was applied to the troughs and crests of the rails to provide a liquid metal interface that acted as a conductor over the whole projectile area. The projectiles used had physical dimensions very similar to Adamy's.

B. POWER SUPPLY

The major components of power supply, from left to right with respect to the abbreviated schematic seen in Figure 4 below, consists of two 830 μF

capacitors, both rated at 11 kV, configured in parallel and providing a total capacitance of 1660 μF. These capacitors are protected by three strings of six DA24 F2003 high power avalanche diodes, which prevent the current from reversing on the capacitor bank during discharge. The circuit is closed by the TVS-40 vacuum switch, which functions as fast-action switching medium. As a part of Culpeper's thesis, a 30 μH inductor was added between the TVS-40 fast-acting vacuum switch and the rails; the reasoning for this insertion will be discussed in the following section. This inductance combined with the 2.5 μH inherent inductance of the power supply provides a total inductance of 32.5 μH. Culpeper also reconfigured the power supply to allow the voltage across the rails to be measured by adding a 0.03 Ω resistor in parallel with the rails. A differential amplifier was used to display the waveforms obtained to the oscilloscope. This improvement provided definitive data as to how well the projectile was making contact with the rails, while also giving a clearer indication of the exact time the projectile exited the rail test platform.

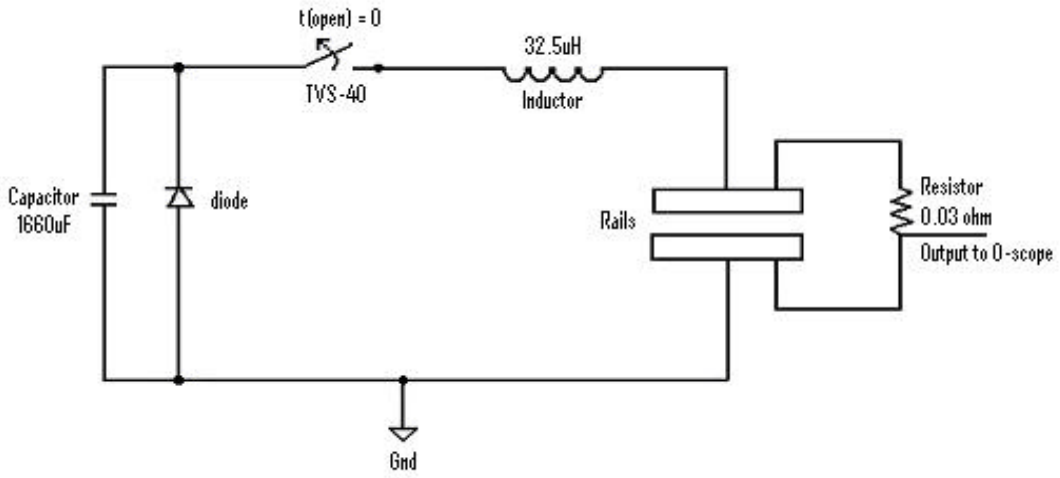

Figure 4. Schematic of the Major Components of the Power Supply

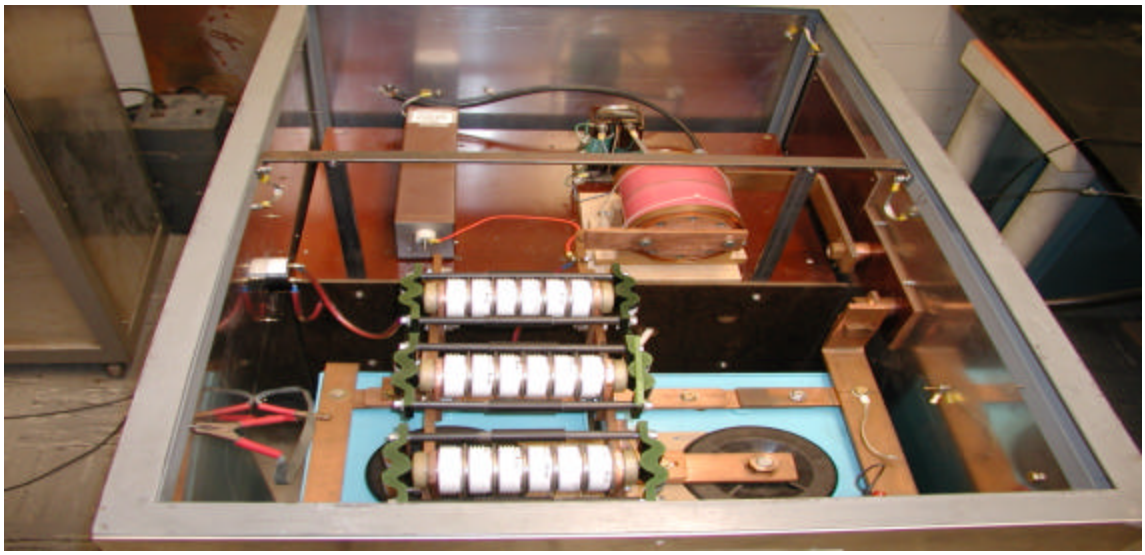

Figure 5. Overhead View of Power Supply

C. ADDED INDUCTANCE

The theoretical curve of current versus time is shown below in Figure 4. Several components of the power supply influence the characteristic curve, specifically; the combined inductance and capacitance dictate the rise time, whereas, the decay is controlled by the combined inductance and resistance [1,6].

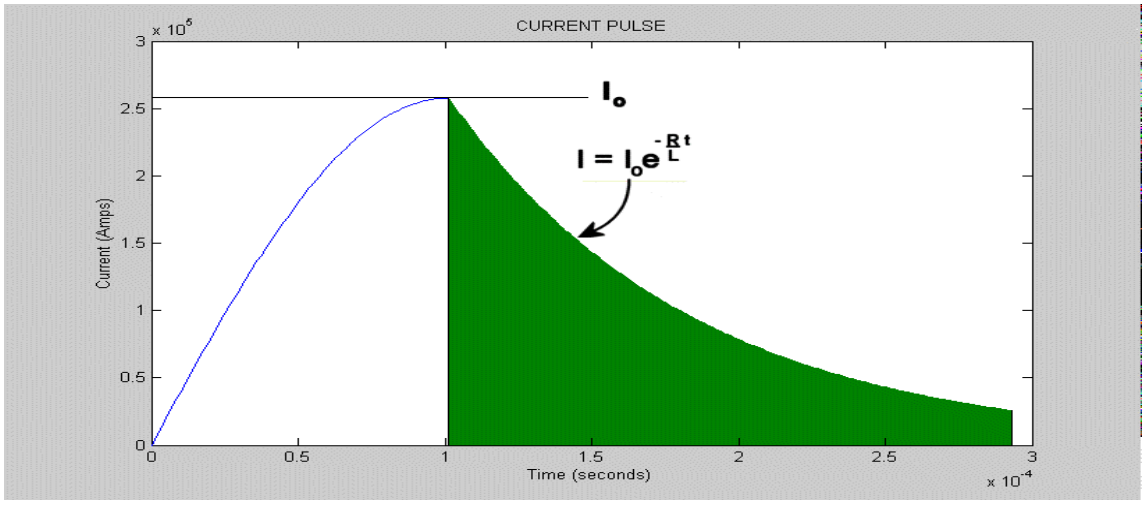

Figure 6. Characteristic Exponential Decay Curve of Current vs. Time, L = 2.5, C = 1660 μH , R = 9 $m\Omega$, Voltage across the Capacitors, V_c = 2.25 kV.

The inherent inductance, 2.5 μH, of the power supply and rail gun produce the short current pulse and characteristic exponential decay curve represented in Figure 6. Although the current is rather large initially, it falls to a low level as the projectile travels along the entire length of the 4-inch rails. In order to increase the decay time of the exponential characteristic, an additional inductance has been added. To ensure that large current values are present throughout the passage of the projectile along the length of the rails, the current pulse is widened by adding about 30 μH to the circuit. The magnitude of the current can be estimated from the following equation:

$$I = I_o e^{\frac{-Rt}{L}} \tag{2.1}$$

The following terms from the above equations are defined as follows:

I = the current value I_o = the peak value of the current

R = the resistance t = the time expressed in seconds

L = the inductance

Culpeper used the following equation to have a 30 μH inductor fabricated and added to the rail gun power supply providing for the optimum impedance match:

$$N = \sqrt{\frac{L(9a + 10b)}{a^2}} \tag{2.2}$$

The following terms from the above equations are defined as follows:

N = the number of turns over the entire coil

a = the radius of the coil

b = the length of the coil

The inductance was placed between the rail gun power supply and the positive rail terminal, which lengthened the decay time of the current pulse to

provide a much better distribution throughout the length of the 4-inch grooved rails [1].

D. CURRENT DENSITY

The fastest method of getting a weapon system approved and implemented aboard Navy vessels is to ensure its operation under the same restrictions and conditions in the laboratory and then carry that same success to the fleet. To ensure that this happens, the current densities anticipated for shipboard use were required of the rail gun test platform. Figure 7 provides a graphical representation of current density as it is displaced through the area of the projectile.

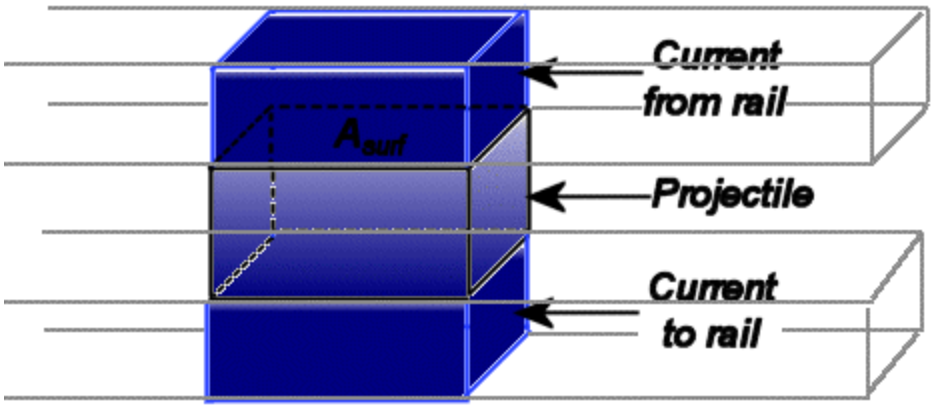

Figure 7. Graphic Representation of Current Density

In order to obtain a physical value for the current, a Pearson Transformer was placed in series between the TVS-40 fast-acting vacuum switch and the total inductance of 32.5 μH. This transformer had a sensitivity of 5 $\frac{mV}{A}$ and was used to generate a waveform on the Oscilloscope.

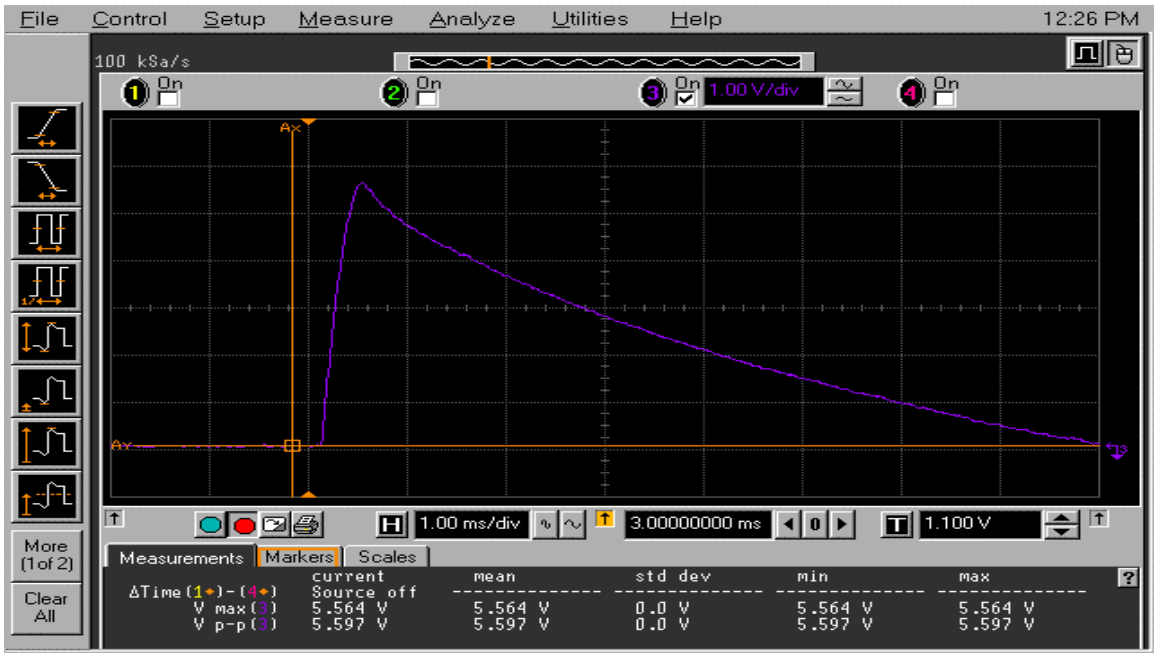

Figure 8. Current pulse. Ordinate scale is 1 V per division. Abscissa scale is 1 ms per division.

In Figure 8, the capacitors were charged to 2.2 kV and then discharged through the 0.03 Ω resistor across the empty rail gun. The peak-to-peak voltage of the current waveform is 5.597 V. A 10:1 voltage divider was connected to the oscilloscope from the Pearson Transformer so that the voltage lies between 5-10 V. From the data mentioned above, the current could be calculated using the following equation.

$$I_{peak} = \frac{V_{p-p} * 10}{\frac{5mV}{A}} = \frac{2000 * V_{p-p}}{\frac{V}{A}} = 2000 * V_{p-p}(A) \qquad (2.3)$$

As mention above, the maximum voltage, $V_{p\text{-}p}$, is 5.597 V. Equation 2.3 yields a peak current of 11.2 kA. When the capacitors are charged to 2.2 kV, approximately 3.6 kJ of energy is in the system [7]. The peak current was divided by the projectile area (0.604 cm^2) to provide an average current density, J , of 18.5 kA/cm^2,

$$J = \frac{I_{peak}}{Area} = \frac{A}{cm^2} \qquad (2.4)$$

Follow-on test were conducted from the 2.2 kV mentioned previously up to approximately 3.8 kV, corresponding to current densities ranging from 18 kA/cm^2 to 32 kA/cm^2, respectively.

E. PARTS

1. Accelerator

Both Adamy and Culpeper used an ME Schermer Captive Bolt Cattle Stunner as a projectile accelerator. Culpeper stated in his thesis that the stunner consists of a 175-gram bolt that extends out of the housing a distance of 7.5 cm when fired, three rubber rings that stop the bolt's momentum, and a small cartridge which is used to accelerate the bolt [1].

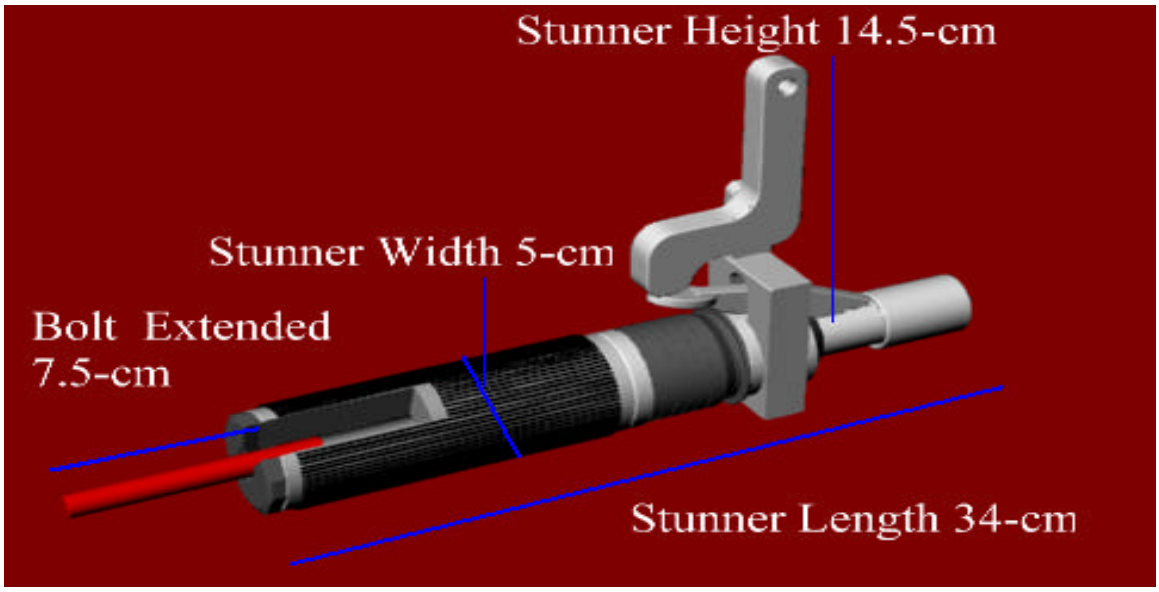

Figure 9. Computer Generated Graphical Representation of the Accelerator

Figure 9 is a graphical representation of the ME Schermer Captive Bolt Cattle Stunner. The cartridge housing is capable of holding four different types of cartridges varying in explosive intensity. The yellow #13 cartridge, which had the smallest charge, was used throughout my experiment. Culpeper measured the

velocity of the captive bolt in order to determine how fast the stunner's bolt traveled when fired with the different cartridges. The stunner was fired five times for each cartridge. The statistical data for yellow #13 showed that captive bolt traveled 5 cm in 1.25 ms, which give an average velocity of 40 m/s with an average deviation of 2 m/s. For an in depth analysis of the velocity of the captive bolt, refer to Culpeper's thesis [1].

2. Pusher Housing

The pusher housing consists of two parts: 1) the pusher assembly which lies in the interior region, and 2) two ports mounted on the exterior region for the attachment of fiber optic cables. The pusher interrupts a beam of light between the fiber optic cables; this interruption causes the TVS-40 fast-acting vacuum switch to conduct and then discharges the capacitor bank after the cattle stunner is fired. For greater details on the pusher housing refer to Adamy's thesis [2]. Figure 10 below shows the base of steel support of the pusher assembly within the pusher housing.

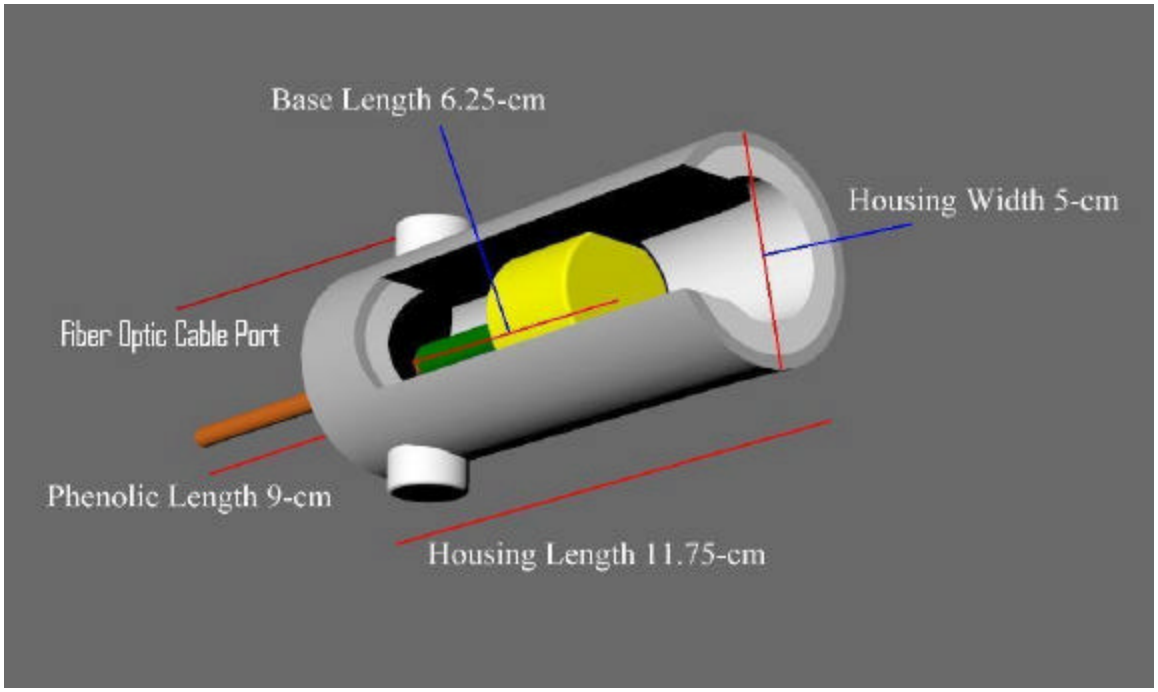

Figure 10. Pusher Housing with Dimensions

3. Pusher Assembly

The pusher assembly consists of two parts: 1) the base piece, and 2) a 9 cm linen filled phenolic rod having one-quarter inch diameter. The length of the phenolic rod was chosen so that it would only have to push the projectile a distance of 0.25-in to accelerate the projectile from its initial position. The base piece is a circular disk composed of hardened aluminum with a steel cylinder support to which the phenolic rod is attached. To ensure minimal damage is sustained by the rail gun test platform when the stunner is fired, an aluminum disk is placed between the captive bolt and the pusher assembly to minimize damage to the pusher base piece, and two 0.125-in thick neoprene disks sit around the metal rod portion of the pusher assembly base piece to minimize damage to the interior of the housing assembly.

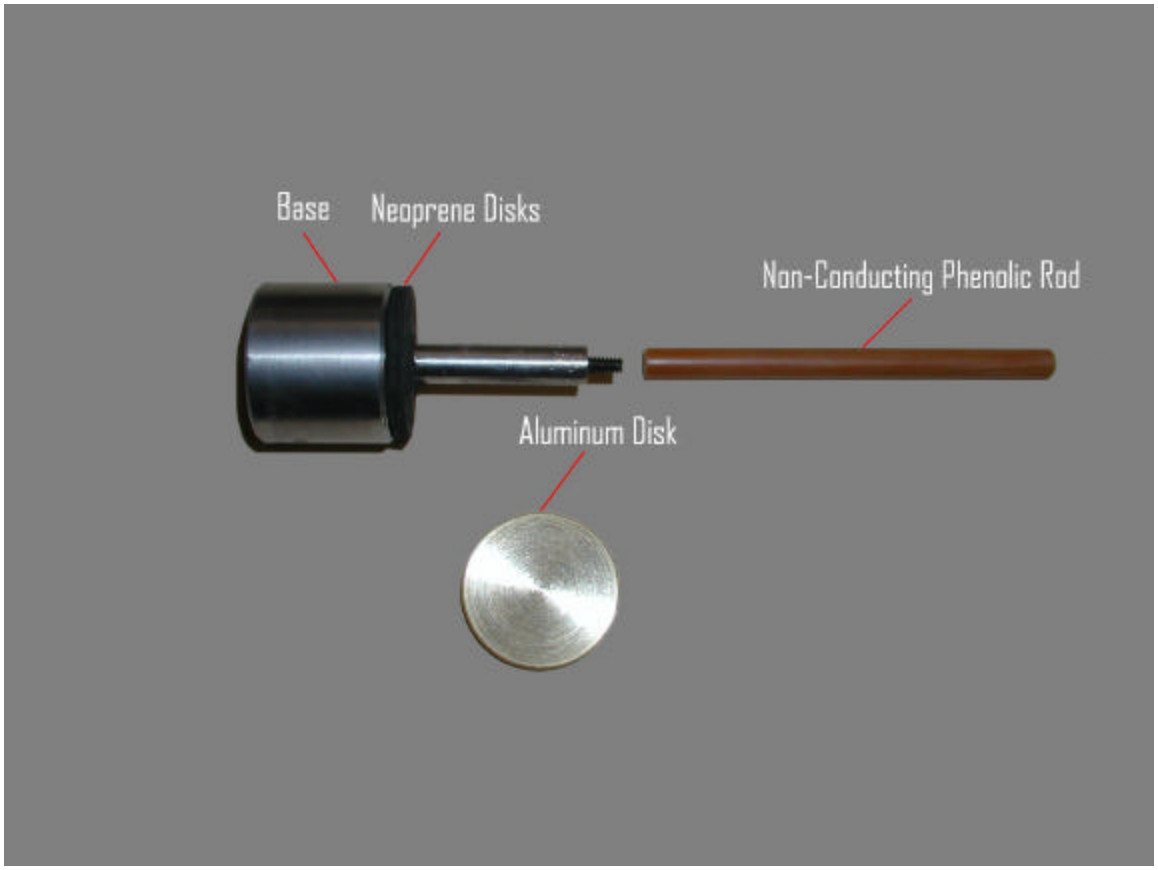

Figure 11. Pusher Assembly with Aluminum and Neoprene disks

F. TRIGGER BOX AND DELAY GENERATOR

As mentioned in Culpeper's thesis, the "Delay Generator" used in the rail gun lab is a Four Channel Digital Delay/Pulse Generator, model DG 535, built by Stanford Research Systems Incorporated. After the leading edge of the pusher assembly breaks the light beam between the two fiber optic cables attached to the pusher housing, a signal is sent to the delay generator via the trigger box. The delay generator sends a signal to the TVS-40 fast-acting vacuum switch, which causes the switch to close and discharges the capacitor bank [1].

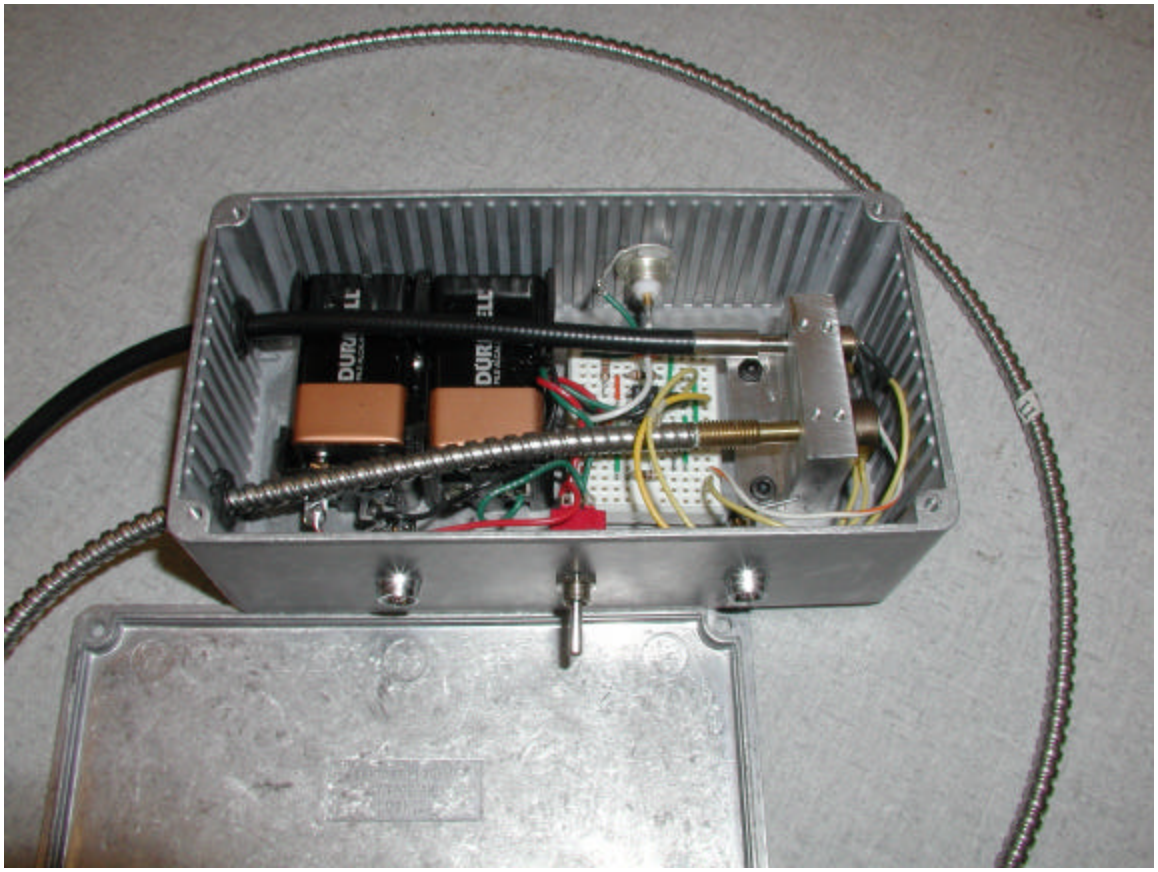

Figure 12. Trigger Box with Fiber Optic Cables

Figure 13. Model DG535 Four Channel Digital Delay/Pulse Generator

G. DIFFERENTIAL AMPLIFIER

Culpeper's thesis suggested that the voltage across the rails should be sent into a fully isolated differential amplifier, and the output from the amplifier be fed into the oscilloscope in order to monitor capacitor voltage, current, voltage across the rails, and provide a possible clear indication of when the projectile exits the rail platform [1]. For this reason, The Lecroy DA1822A Differential Amplifier was purchased and connected in parallel with the 0.03 Ω resistor and the rails.

Figure 14. Lecroy DA1822A Differential Amplifier

H. VARIABLE GRAPHITE RESISTOR

The Lecroy DA1822A Differential Amplifier was connected in parallel across both ends of a variable graphite resistor. The resistor made it possible to obtain the voltage drop across the rails, while the differential amplifier reduced common-mode electrical pickup enough to allow the signal to be displayed on the oscilloscope in real time. The resistor is a variable compressible resistor consisting of graphite squares stacked together and compressed in a vice. Tightening the vice decreases the resistance, while loosening the vice increases the resistance. Two sheets of phenolic lined the resistor to prevent the graphite from coming into contact with the steel housing. To enable the resistor to act as a 10:1 voltage divider, a thin square brass piece was inserted between two of the graphite plates. Figure 15 below provides a visual representation of how the resistor was configured in respect to the rail gun test platform. For a schematic overview of the placement of the resistor, refer to Figure 4.

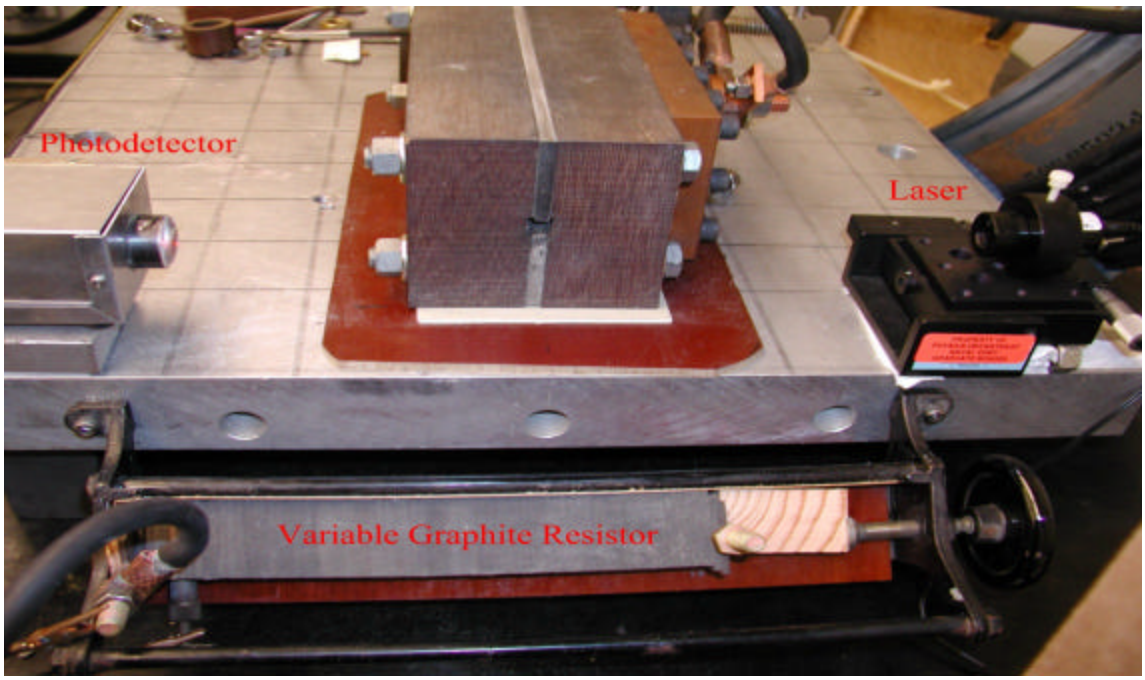

Figure 15. Laser, Photodetector, and Variable Graphite Resistor

The decision to mount the resistor in front of the rail gun was based on the need to prevent inductive pickup from the large fluctuating magnetic fields by keeping the leads connecting the resistor to the rail poles as short as possible, in this case approximately 13-in apiece. The addition of the Lecroy DA1822A Differential Amplifier improved the quality of data collected from that incorporated in Culpeper's thesis, where an analog Oscilloscope was used in conjunction with a digital camera relayed to a computer [1].

I. VELOCITY MEASUREMENTS WITH THE DIFFERENTIAL AMPLIFIER

Culpeper's thesis incorporated a simple design that used a diode laser and a photo-detector device to determine the velocity of the projectile as it exited the barrel. The laser was placed directly across from the photo-detector on either side of the rail gun platform approximately 1 cm ahead of the bore, as seen in Figure 15.

The basic operation of the laser for velocity measurements is initiated when the Schermer Captive Bolt Cattle Stunner is fired. The bolt hits the pusher assembly and drives it into the base of the pusher housing. The motion of the pusher base interrupts the beam of light between the fiber optic cables, which in turn triggers the TVS-40 fast acting vacuum switch to conduct. The capacitor bank then discharges into the rails. Once the pusher assembly travels the full length of its course, the projectile, which began against the non-conducting phenolic rod is accelerated to a velocity of about 34 $\pm$ 19 m/s. The projectile exits the rails and breaks the beam of light between the laser and photo-detector. The capacitor bank discharge acts as initial waveform and the interruption between the laser and the photo-detector serves as a final waveform to determine the time between start and projectile emergence from the rail gun test platform. The distance that the projectile travels is divided by the time difference to obtain a velocity. For a schematic representation of the laser setup, refer to Figure 16. During this thesis work, the laser data was found to be sometimes inconsistent with the current data and were thought to be unreliable. Current

data shows distinct changes when the projectile emerges from the rails, and the voltage across the rails is a sensitive measure of changes in electrical resistance, i.e. of electrical contact.

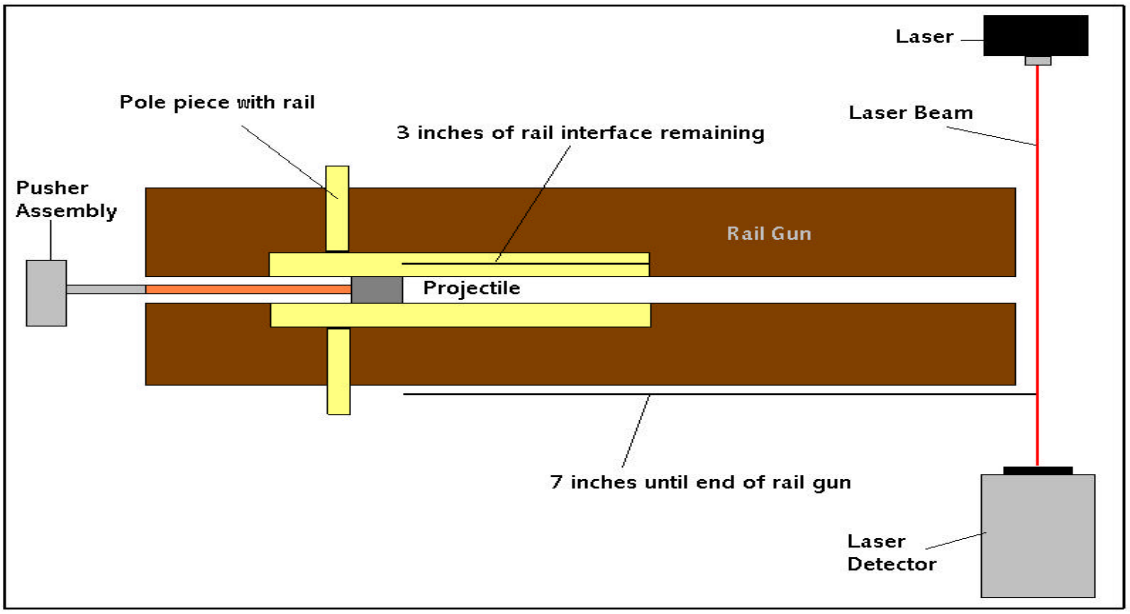

Figure 16. Laser Setup of the Rail Gun Test Platform

Note: Figure 16 indicates the exact placement of the projectile inside the rail gun test platform.

III. TEST RESULTS

A. PROJECTILE VELOCITY RESULTS

Figure 17 represents a test shot taken at a capacitor bank charge of 3 kV. The A_x marker indicates when the pusher base breaking the beam of light between the two fiber optic cable ports while the B_x marker indicates when the current indicated that the projectile exited the rails. Waveform 1 (yellow) corresponds to the trigger received by the fiber optic cables, which is relayed to the pulse generator that causes the TVS-40 to conduct. Waveform 2 (green) corresponds to the signal received from the interruption of light between the laser and photo-detector at the exit end of the rail gun test platform. Waveform 3 (purple) corresponds to the voltage from the Pearson Transformer (i.e., to the current through the rails), while waveform 4 (maroon) corresponds to the voltage developed across the 0.03 Ω resistor and fed to the oscilloscope via the differential amplifier. This description of the waveforms and their respective colors will stay consistent throughout my thesis. The difference in time (Δt) between the markers Ax and Bx is approximately 3.82 ms. The total distance the projectile travels between the rails is 3-in (0.0762 m). The velocity can be calculated by dividing the distance (Δl) by the time (Δt) and is approximately 20 m/s. The average velocities were found to be 34 $\pm$ 19 m/s. We had trouble getting the laser beam to detect the projectile consistently; therefore, the time between the fall of the yellow curve and the transition determined from the maroon curve will be used to calculate projectile speed.

The inconsistencies between Δt obtained from the maroon and green curves can be seen in Figures 17-19. In Figure 17, the projectile was accelerated when the yellow curve fell. The projectile exited the rails and transitioned from sliding contact to discharge when the maroon curve rose. The green curve indicates that the projectile did not interrupt the laser beam, which was interrupted by debris following the projectile.

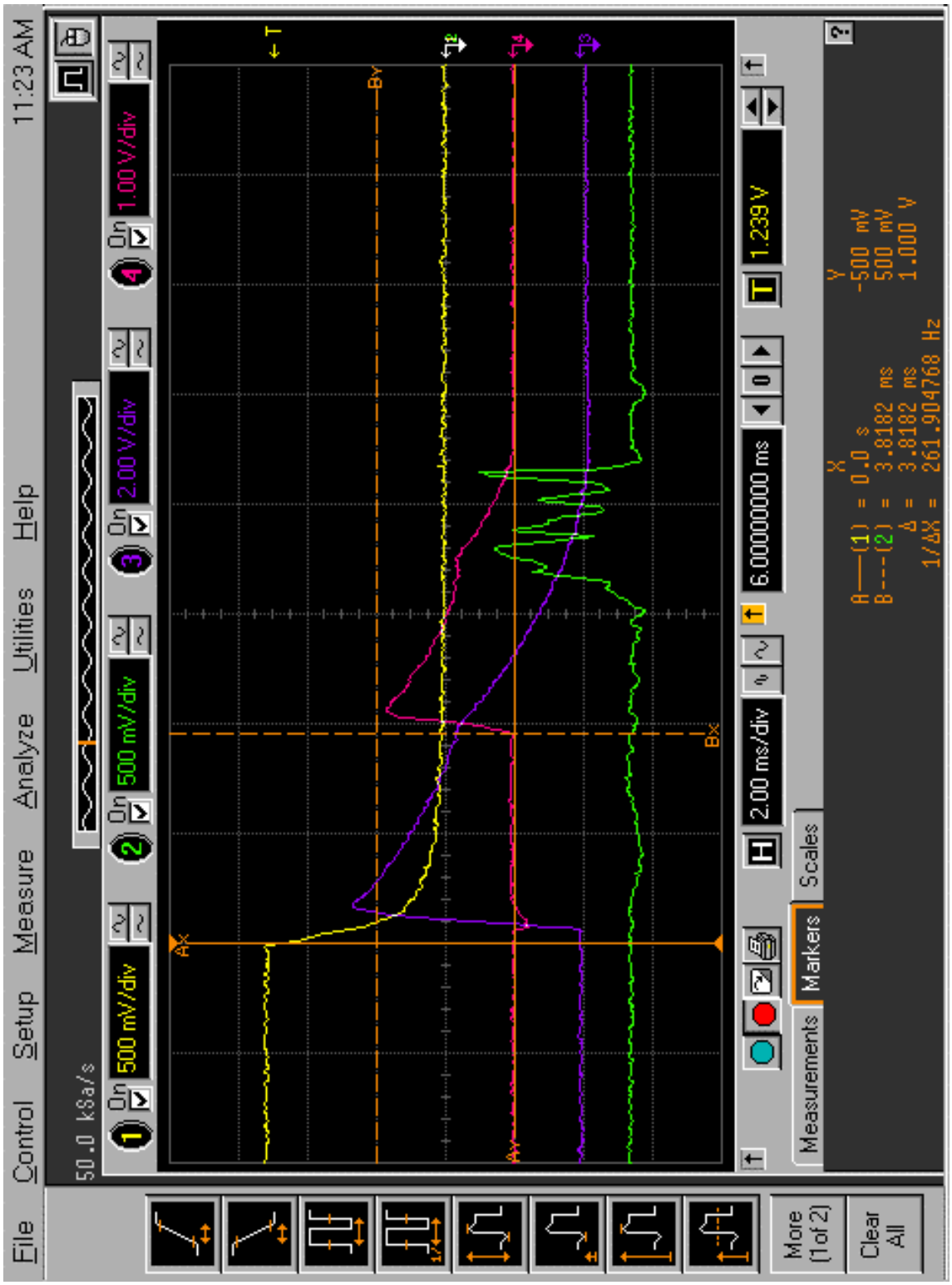

Figure 17. Delta Time at 3 kV Capacitor Charge. Ordinate scale is as indicated by the color associated with each waveform. Abscissa scale is 2 ms per division.

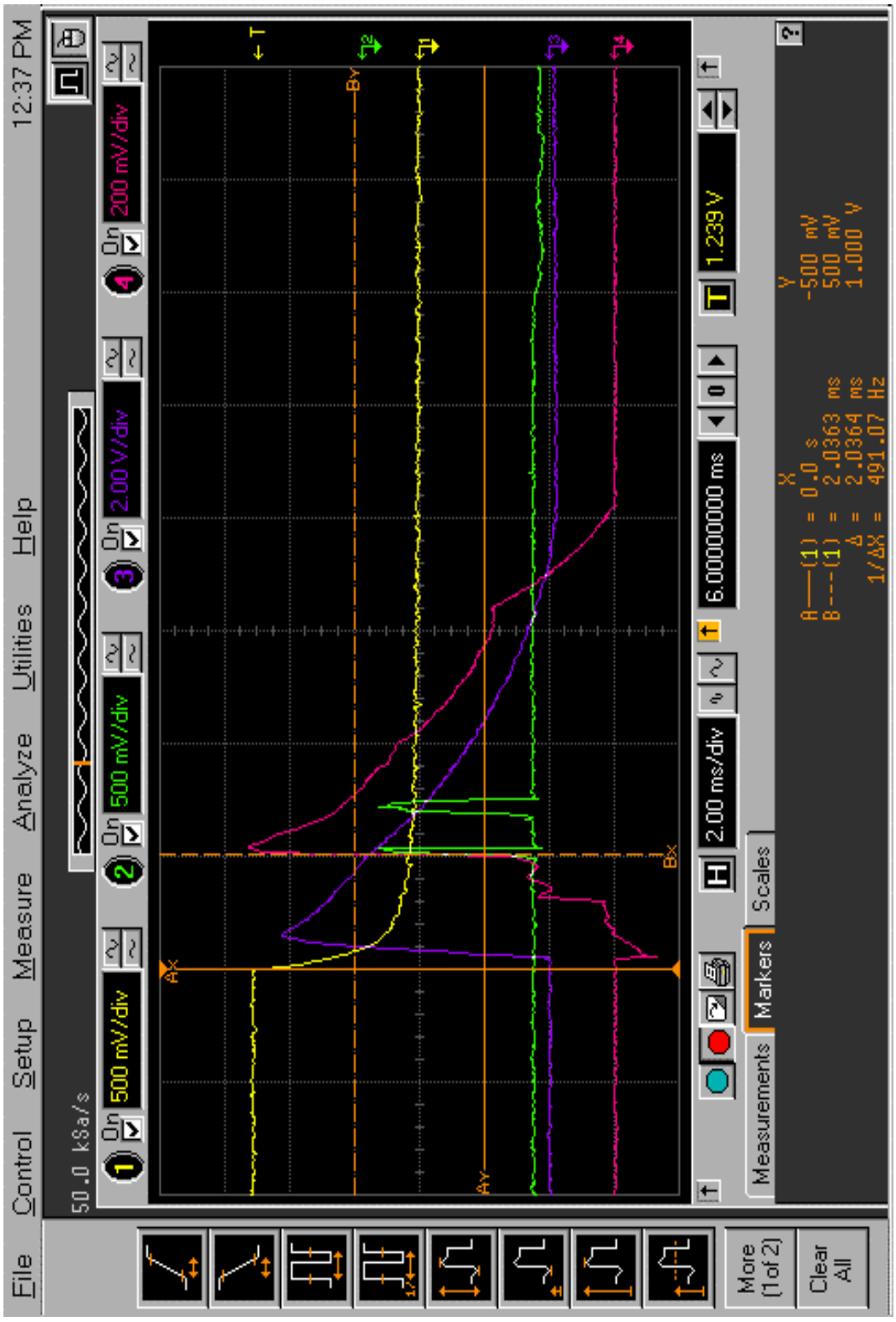

Figure 18. Delta Time at 3.6 kV Capacitor Charge. Ordinate scale is as indicated by the color associated with each waveform. Abscissa scale is 2 ms per division.

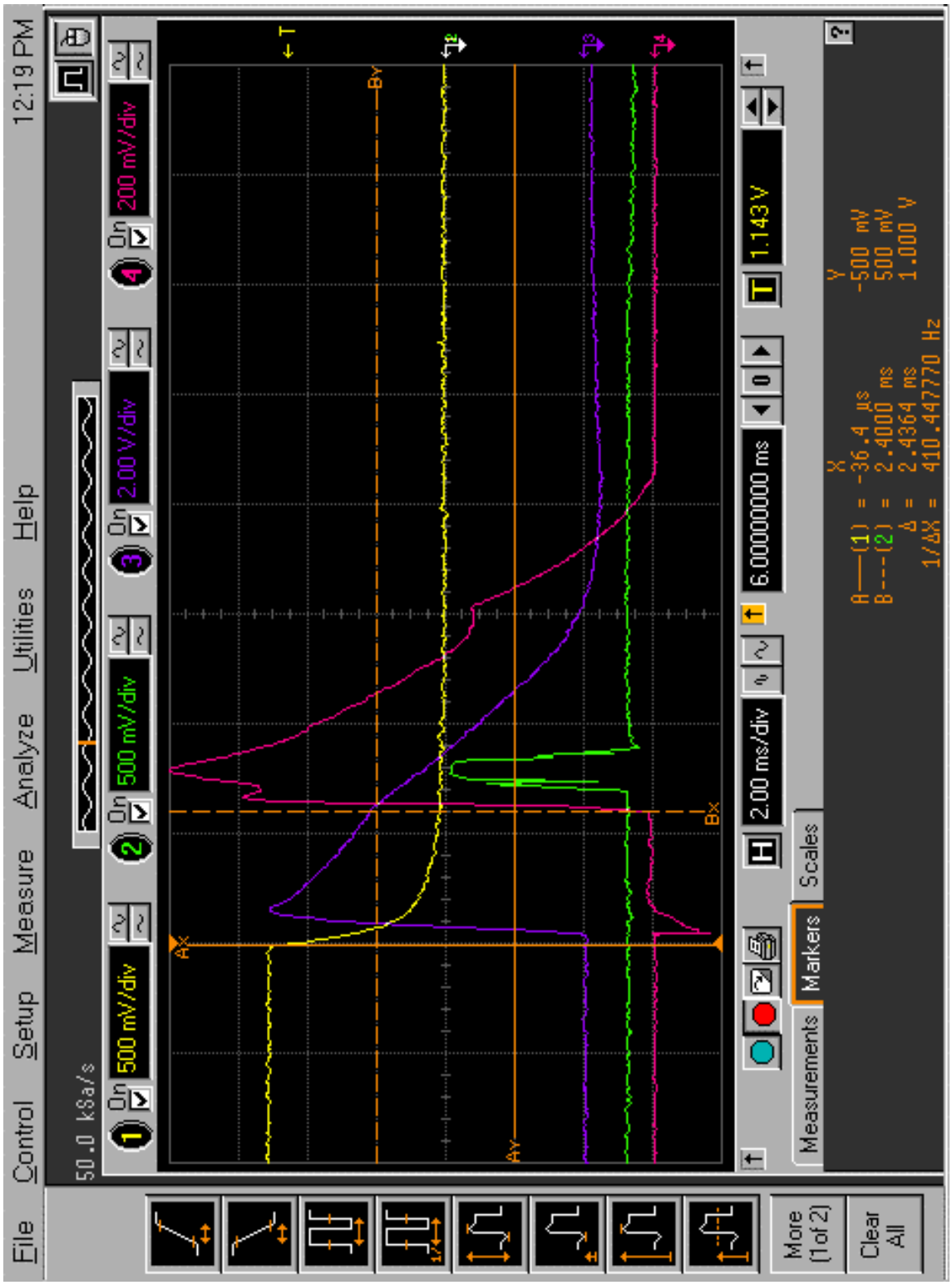

Figure 19. Delta Time at 3.8 kV Capacitor Charge. Ordinate scale is as indicated by the color associated with each waveform. Abscissa scale is 2 ms per division.

Capacitor Voltage	Shot Number	Vp-p (a)	Laser (b) Delta Time	Diff. Amp. (c.) Delta Time	v (d) Laser	v (e) Diff. Amp	v avg. Laser	v avg. Diff. Amp.
2200	1	5.597	0	1.4545	X	52.39	X	53.41
	2	X	0	1.4	X	54.43		
2400	1	X	2.0364	1.8	87.31	42.33	91.59	41.71
	2	5.51	1.8545	1.8545	95.87	41.09		
2600	1	6.12	2.9455	2	60.36	38.1	80.08	44.45
	2	6.11	1.7818	1.5	99.79	50.8		
2800	1	6.65	X	X	X	X	47.01	20.15
	2	6.37	3.7818	3.7818	47.01	20.15		
3000	1	6.89	6.3	3.8182	28.22	19.96	31.89	24.53
	2	X	5	2.6182	35.56	29.1		
3300	1	7.95	2.1	2.8364	84.67	26.87	84.67	35.27
	2	7.75	0	1.7455	X	43.66		
3600	1	8.6	1.8545	1.8545	95.87	41.09	91.59	39.26
	2	8.51	2.0364	2.0364	87.31	37.42		
3800	1	9.12	1.9	2.1455	93.58	35.52	82.35	33.4
	2	9.66	2.5	2.4364	71.12	31.28		

(a) Data taken from Figs. 17-19 and similar plots
(b) Delta t computed from green curves in Figs. 17-19 and similar plots
(c.) Delta t computed from maroon curves in Figs. 17-19 and similar plots
(d) Delta l for the laser is 7"
(e) Delta l for the differential amplifier is 3"
X - Data was unable to be obtained in these instances

Table 2. Data Table for Velocity.

V	Laser (v)	D. Amp (v)
2200	0	53.41
2400	91.59	41.71
2600	80.08	44.45
2800	47.01	20.15
3000	31.89	24.53
3300	84.67	35.27
3600	91.59	39.26
3800	82.35	33.4

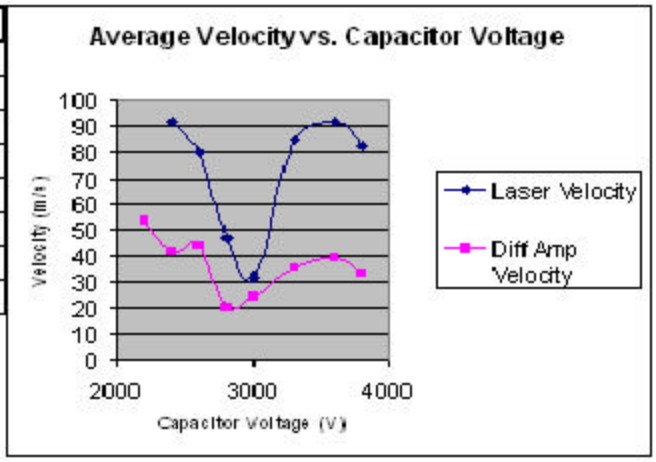

Figure 20. Plot of Average Velocity vs. Capacitor Charge Voltage

Figure 20 illustrates the average velocity of the projectile calculated from times Δt_1, and Δt_2. There is no evidence that the projectile was significantly accelerated by the electromagnetic force in this experiment. Presumably the electromagnetic force was less than or near to the frictional forces between the projectile and rails.

Variations observed in projectile exit velocities were attributed mainly to inadequate control of the spacing between the rails. As seen in Figure 21, rail spacing depends on how the twelve bolts that hold the rails in place are tightened, and we have inadequate control at this time. To ensure conductivity from the rail post through the projectile to the opposite rail post, an ohmmeter was used to obtain a short circuit, but the bolts had to be loose enough so that the projectile did not become lodged somewhere along the length of the rails when the cattle stunner was fired. Rail spacing was not measured directly.

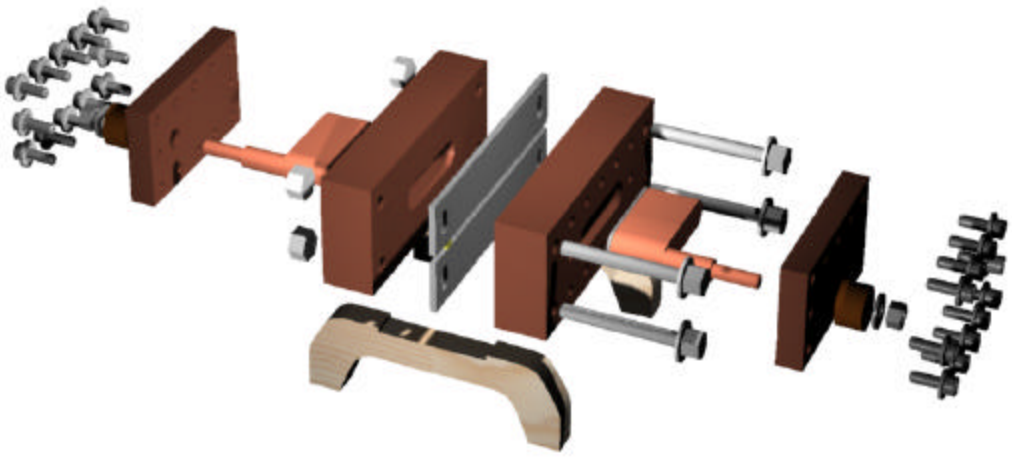

Figure 21. Expanded View of Rail Gun Test Platform

B. UNIFORM CONTACT BETWEEN PROJECTILE AND RAILS

Barrel wear can be minimized provided uniform contact can be maintained between the projectile and rails. Uniform contact minimizes deposition and transition due to the arcing associated with electrical heating. In Figure 22, the maroon line corresponds with waveform 4 and the signal gathered by the differential amplifier. The flatness seen before the projectile exits the rails indicates that at least good electrical contact was maintained throughout the passage of the projectile along the rails.

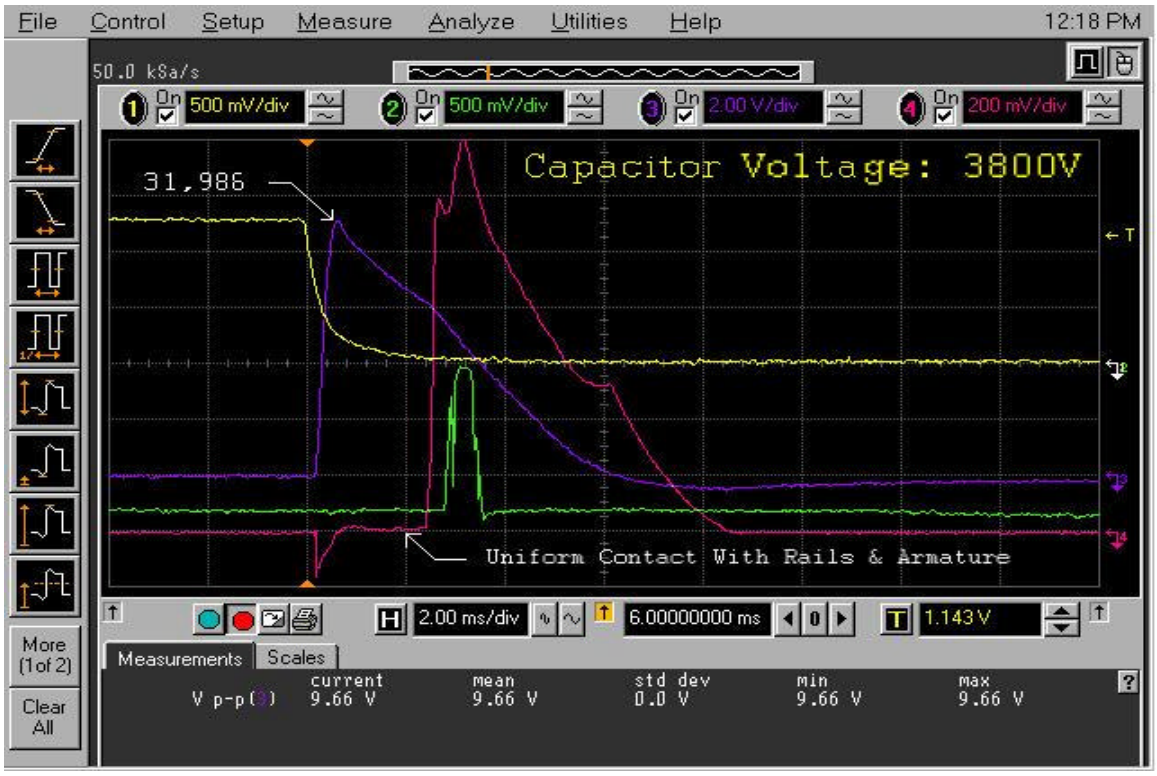

Figure 22. Uniform Contact Between Projectile and Rails. Peak Current = 19.3 kA, J = 32 kA/cm^2

C. NON-UNIFORM CONTACT BETWEEN PROJECTILE AND RAILS

In Figure 23, the fluctuation in the flatness of the maroon line before the sharp increase in the waveform indicates the projectile exiting the rails, which illustrates non-uniform contact. At that point, electrical contact has transitioned to an arc, which damages both projectile and rails.

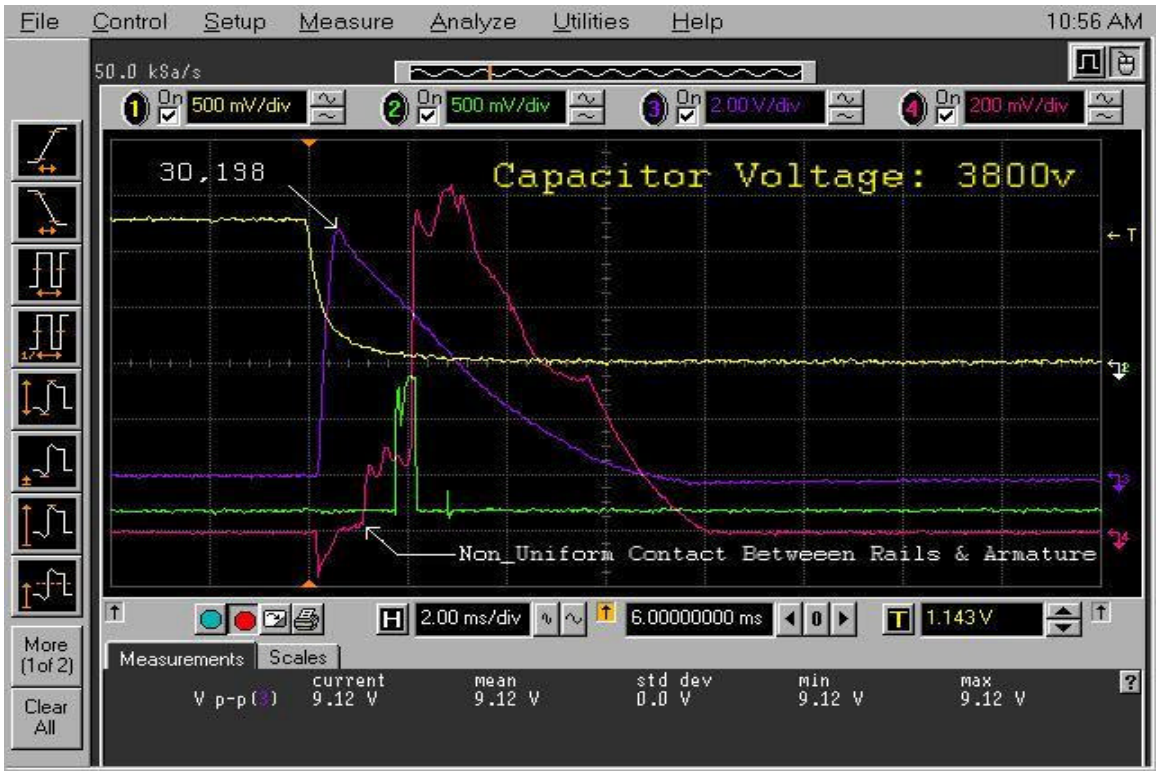

Figure 23. Non-Uniform Contact Between Projectile and Rails. Peak Current = 18.2 kA, J = 30.2 kA/cm^2

For the purpose of this thesis, it was convenient to have a plot of the peak current densities averaged over the conducting surface of the projectile, verses initial capacitor voltage. We read the peak currents from Figures 17-19 and similar plots and divided them by 0.604 cm^2 to obtain a peak average current density, J (A/cm^2). Figure 24 compares the values measured for J with those calculated from Equation 3.1.

$$y = 8.361x - 1729.3 \quad (3.1)$$

The following terms from the above equation are defined as follows:

y = J expressed in units of A/cm^2

x = the capacitor bank charge voltage expressed in V

	Actual	Calculated
V	J	J
2400	18219.77	18336.14
2600	20236.84	20008.26
2800	21989.38	21680.38
3000	22782.98	23352.5
3300	25957.39	25860.68
3600	28305.12	28368.86
3800	31049.66	30040.98

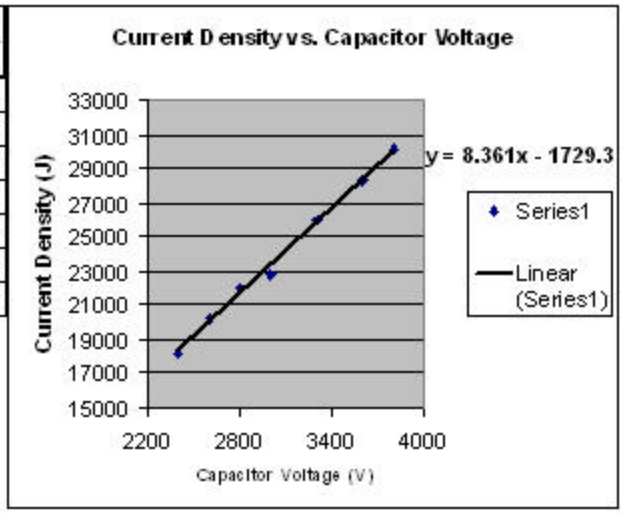

Figure 24. Plot of Current Density J (A/cm^2) vs. Capacitor Voltage

Note: Measured J deviated by less than 1% from J calculated in Equation 3.1.

D. THE SILVER PASTE AS AN INTERFACE MATERIAL

Once the range of projectile velocities had been established for this thesis, the next objective was to find an indication of the current density at which the silver paste that we used as an interface between projectile and rails starts to break down. The capacitor voltage was increased from 2 kV to 3 kV in 200 V intervals and two shots were taken at each voltage. From 3 kV to 3.6 kV, the voltage was increased in 300 V steps. At a capacitor bank voltage of 3.8 kV until a trend line could be established; we reached 32 kA/cm^2 at a capacitor bank charge of 3.8 kV. The rails were coated with silver paste for each firing and then cleaned to determine the amount of damage sustained.

Note: There was concern that the increased voltages and currents might cause the 30 μH inductor to fail.

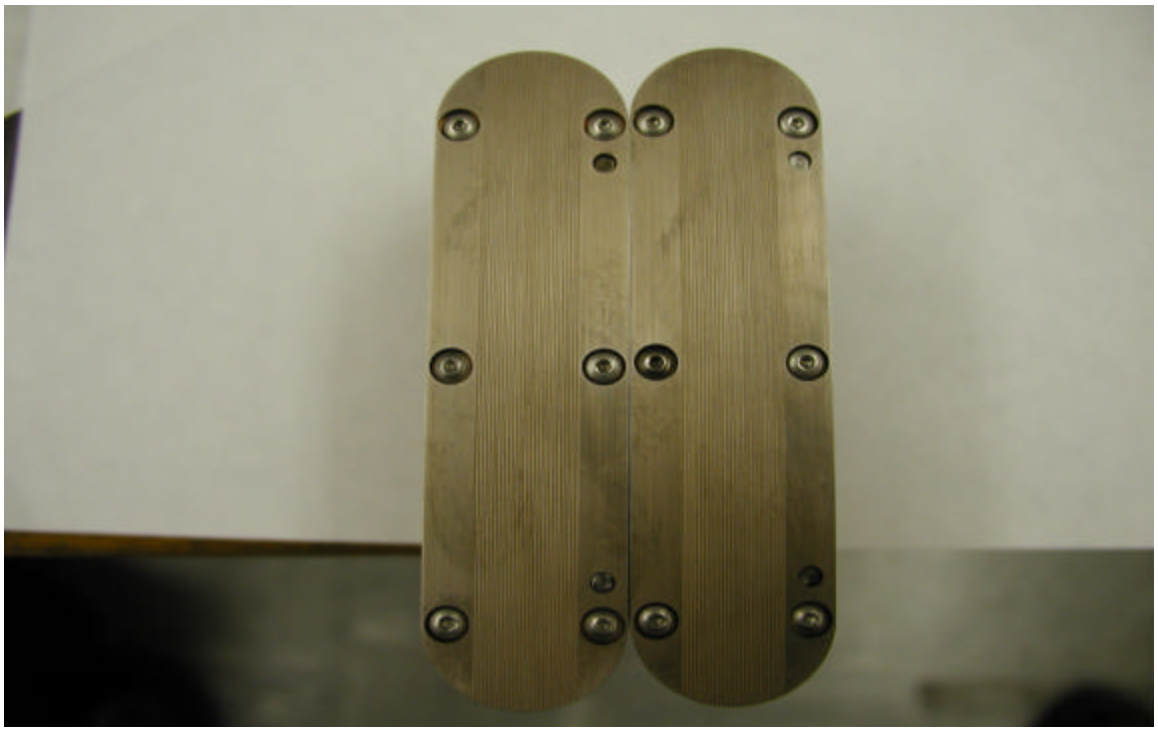

Figure 25. New Rail Prior to First Use

New rails, as seen in Figure 25, were used for successive shots of increasing capacitor bank charge until any form of damaged was noticed. Once the damage was found, new rails were again used to determine if the damage was developed due to repeated use or if the current was sufficient enough to cause damage on the first shot. Before the rails were used in an actual firing of any kind, the silver paste was applied on the portions of the rail that would come in contact with the projectile as seen in Figure 26. The amount of silver paste applied was decided by ensuring that the troughs were filled enough to meet the crests. The intent was to ensure that no part of the rail was in direct contact with the projectile except via the silver paste.

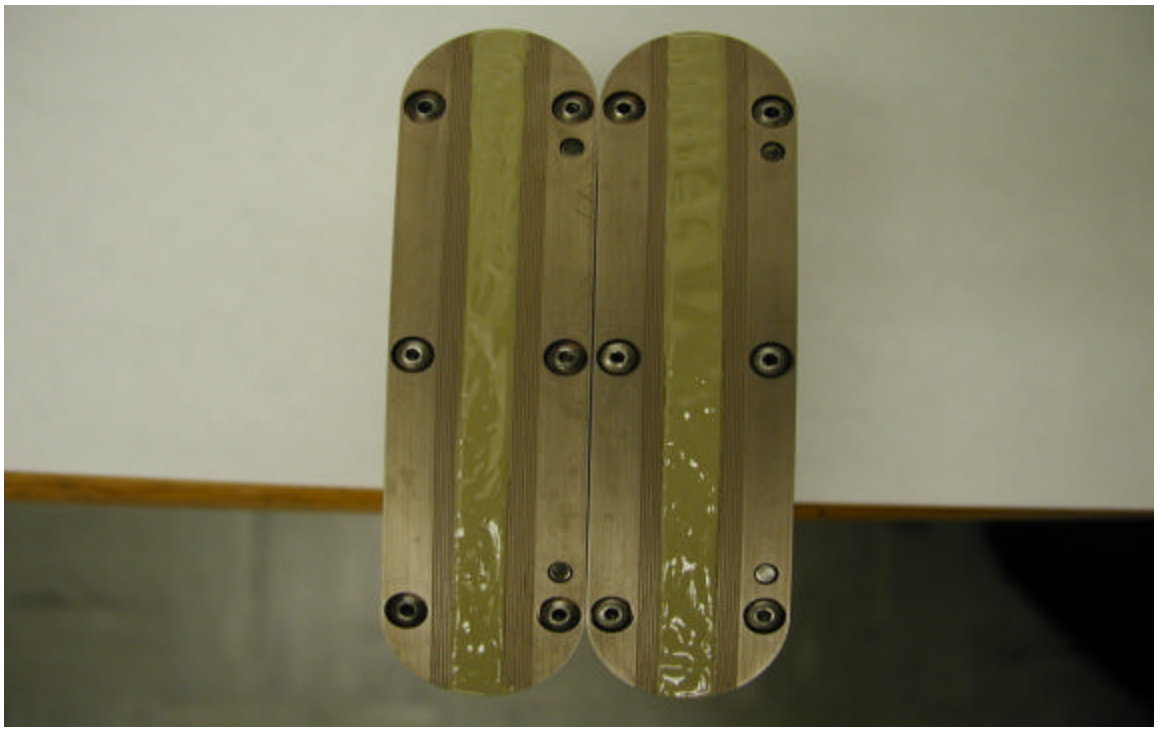

Figure 26. New Rail with Silver Paste Applied

The initial indication of possible breakdown of the silver paste was seen at a capacitor bank charge of 2.8 kV. Figure 27 shows the general blackened condition of the rails and the projectile after one shot. The arc that develops when the projectile exits the rails and breaks direct contact causes most or all of this blackening. This arc damages the back of the projectile and ends of the rails. The $V_{p\text{-}p}$ value was 6.65 V, and we used Equation 2.3 to calculate the peak current of 13.3 kA. Then, Equation 2.4 gives a peak current density, J = 22 kA/cm^2.

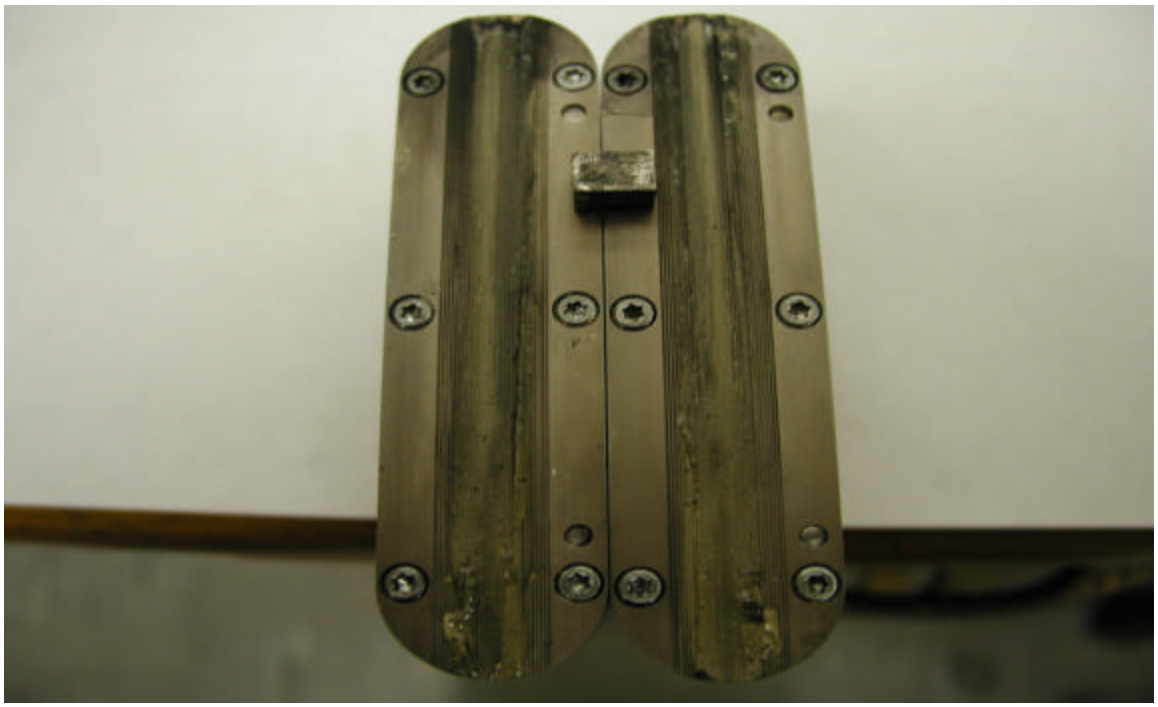

Figure 27. Typical Appearance of Rails with Silver Paste Applied After a Shot. The projectile is also shown. Peak Current = 13.3 kA, J = 22 kA/cm^2.

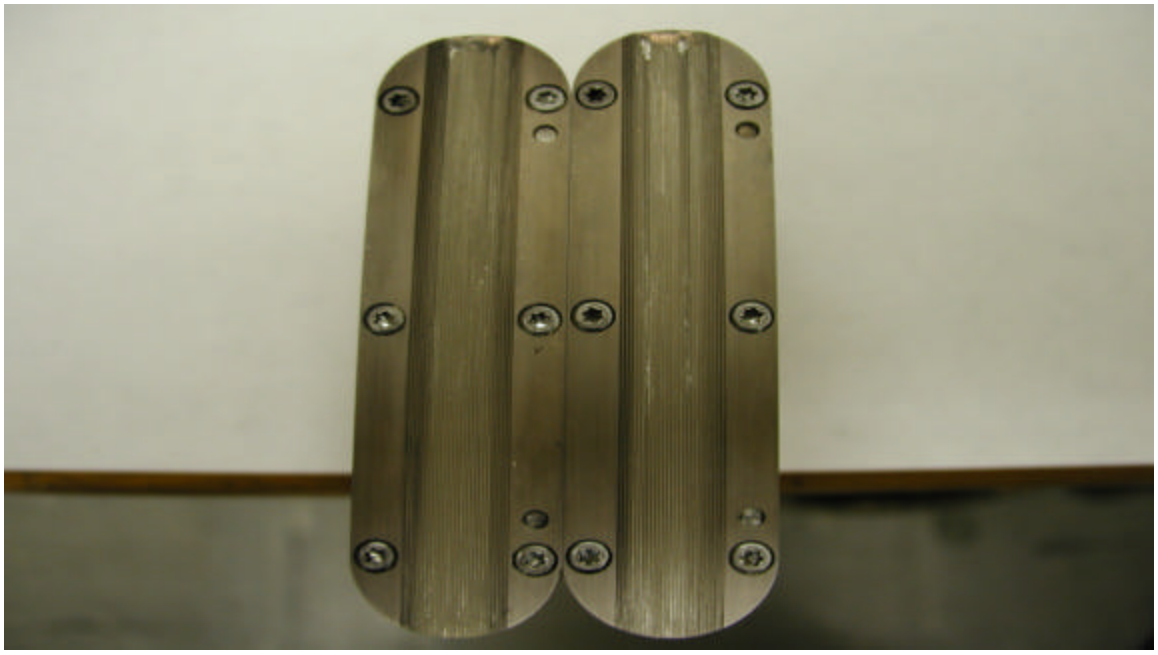

Figure 28. Results After 2.8 kV Shot with Silver Paste Removed. Peak Current = 13.3 kA, J = 22 kA/cm^2. An indication of silver deposit can be seen on the right-hand rail.

Figure 28 shows the rails after the silver paste has been wiped off. The capacitor bank was charged to 2.8 kV were trace deposits of silver was found in some of the grooves. This deposition was sustained after only one shot at this voltage level. Although damage is present, it is minimal.

Figures 29 - 31 show photographs of the rails after several shots were taken at various capacitor voltages. In each case, the paste has been wiped off.

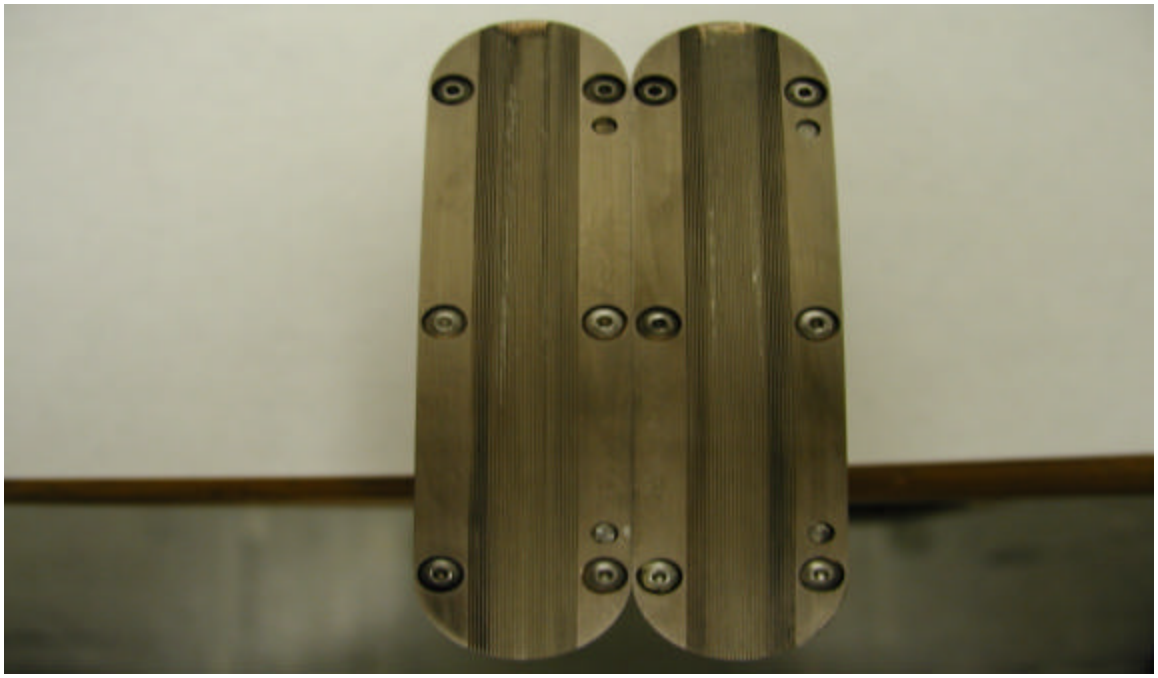

Figure 29. Results After 3.0 kV Shot with Silver Paste Removed. Peak Current = 13.8 kA, J = 22.8 kA/cm^2

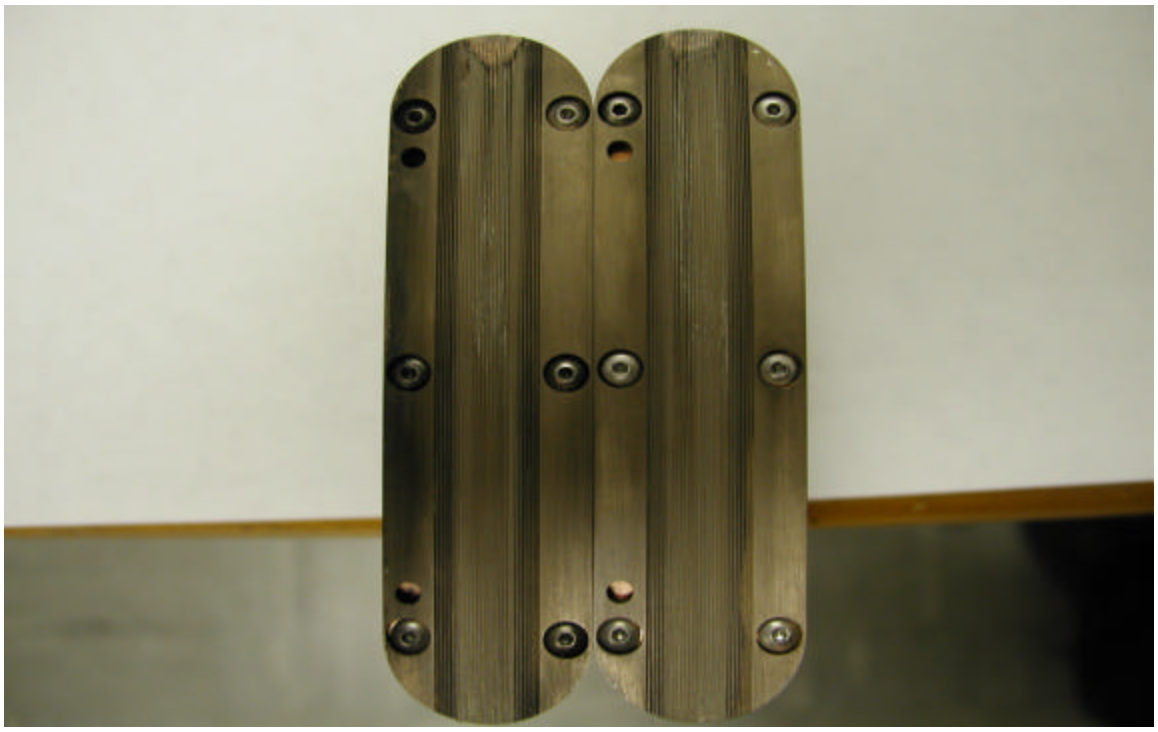

Figure 30. Results After 3.3 kV Shot with Silver Paste Removed. Peak Current = 15.5 kA, J = 25.7 kA/cm^2

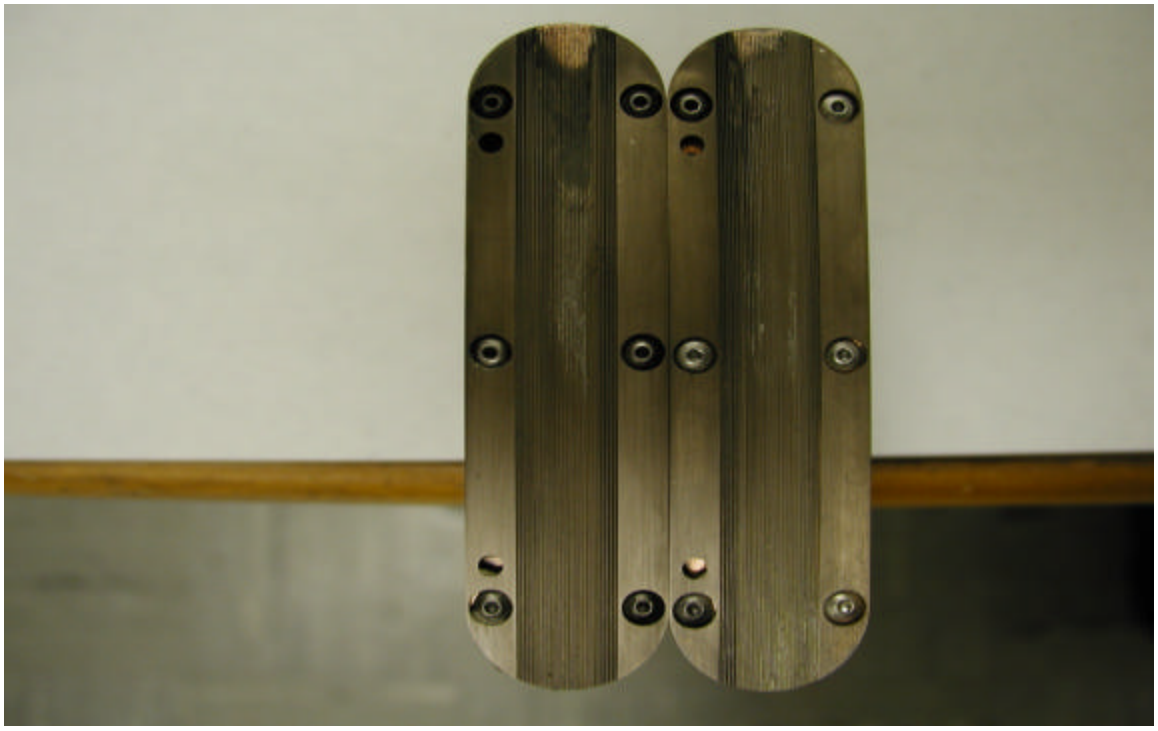

Figure 31. Results After 3.6 kV Shot with Silver Paste Removed. Peak Current = 17.2 kA, J = 28.5 kA/cm^2

Figures 32 and 33 show the rails after a shot at a capacitor voltage of 3.8 kV, corresponding to a peak current of 18.2 kA, i.e. J = 30.2 kA/cm^2. The silver paste in Figure 32 is actually burned before the end of the rail, and corresponding damage to the rails can be seen in Figure 33, which indicates that the system transitioned from direct electrical contact to discharge. This transition is also seen in the maroon curve in Figure 23 as the projectile reaches the end of the test platform prior to exiting. Notice that contact was broken on just one of the rails, and the other rail sustained no damage except for minor silver deposits.

J is the peak current density averaged over the whole area (0.604 cm^2) of one side of the projectile in contact with the rail, but the current distribution through the projectile is by no means uniform. It is to be expected that the current is highest at sharp corners and edges. The photographs of the rail in Figures 28 – 31 and Figure 33 show silver deposits precisely where the sharp corners and edges are in contact with the rails.

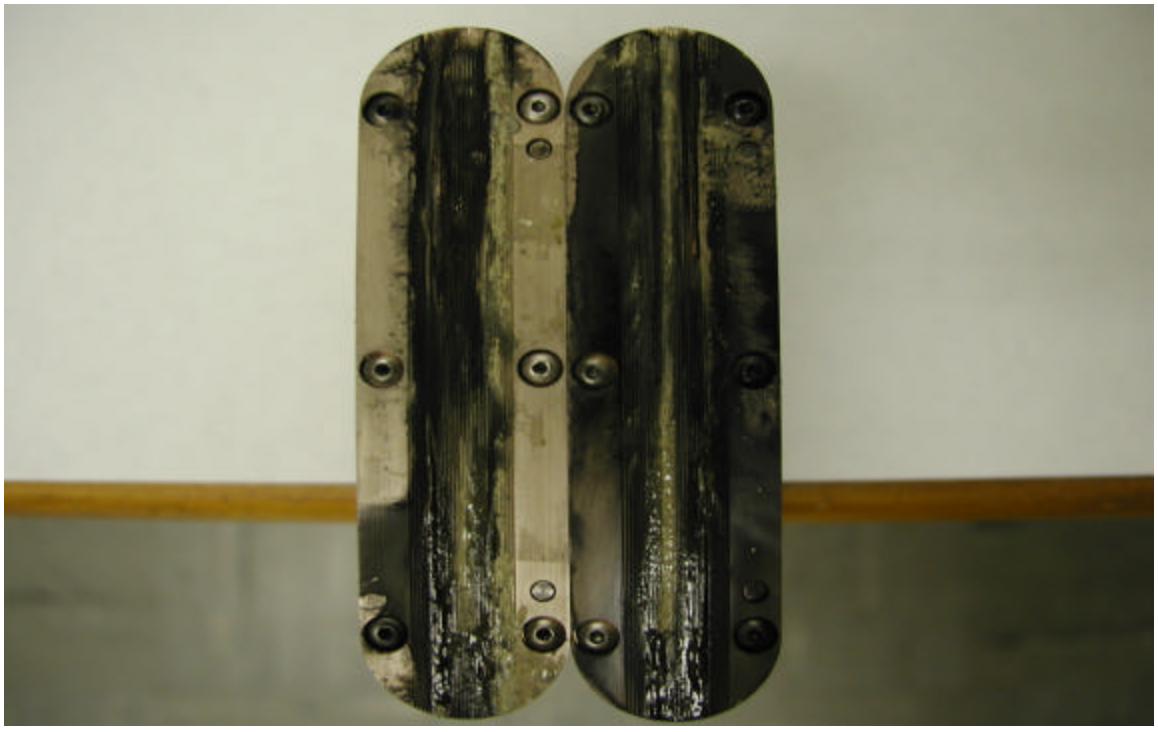

Figure 32. Rails Coated with Silver Paste at 3.8 kV. Peak Current = 18.2 kA, J = 30.2 kA/cm^2.

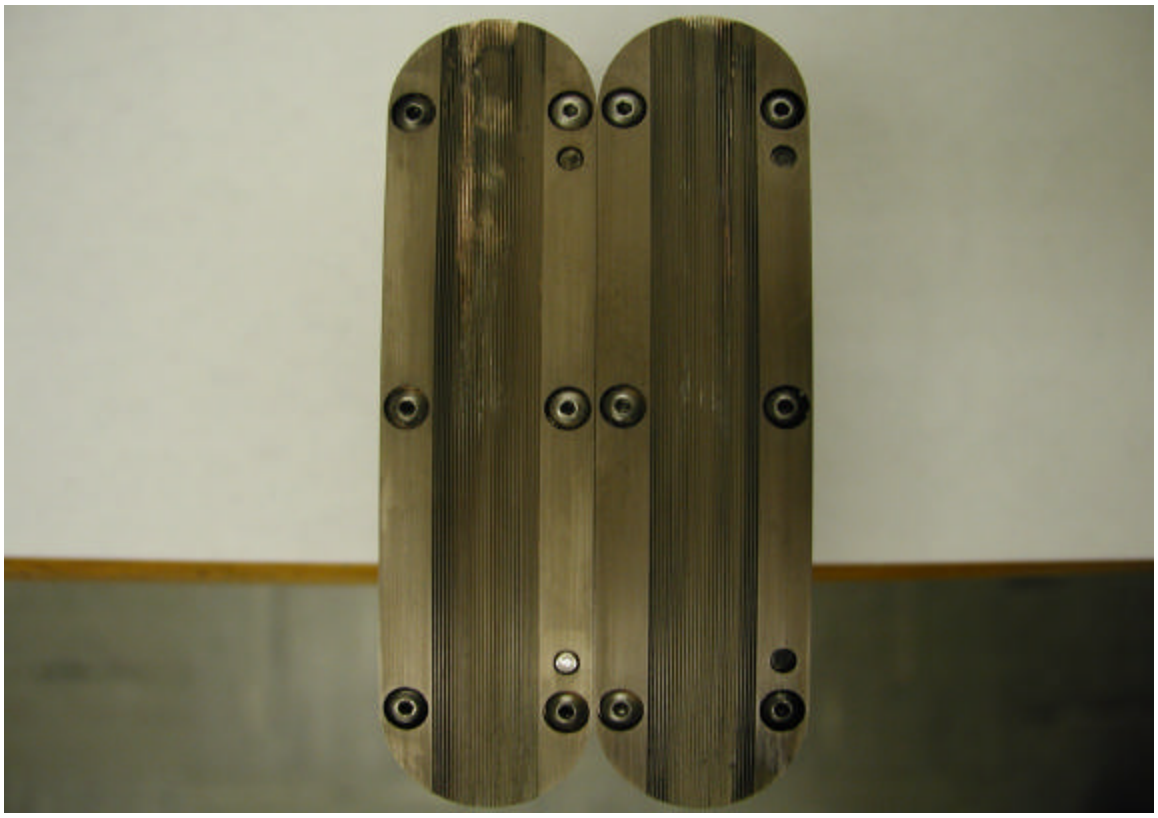

Figure 33. Results After 3.8 kV Shot with Silver Paste Removed. Peak Current = 18.2 kA, J = 30.2 kA/cm^2

THIS PAGE INTENTIONALLY LEFT BLANK

IV. CONCLUSION

The silver paste was very effective in preventing severe damage and erosion to the rails at least for $J \leq 28$ kA/cm^2. Although trace deposits of silver were seen in the grooves of the rails, the rails were still intact and able to be used for successive shots. Although significant rail erosion was observed on one rail for a shot at a capacitor voltage of 3.8 kV (J = 30.2 kA/cm2), the rail separation may have widened toward the exit end of the rails and caused the loss of direct electrical contact that is seen in the maroon curve in Figure 23. Also, the silver deposits on the rails are probably caused by high current densities at the edges and corners of the projectile.

Changes in the apparatus and its operation should be made to permit precise measurement of rail spacing. An improved velocity measurement would also be useful. Finally, additional thought should be given to projectile design to minimize sharp edges and corners in contact with the rails.

THIS PAGE INTENTIONALLY LEFT BLANK

V. FUTURE WORK

This thesis tested the silver paste up to 30 kA/cm^2, but any additional research on the 4-in rail gun test platform should try to achieve greater current densities and greater projectile velocities as well. A more precise method of ensuring consistent rail alignment and parallelism must be determined while also taking the opening and closing of the test platform into consideration. In order to prevent limiting or stopping the projectiles motion along the length of the rails, test platform tightening methods must be found and implemented on every shot. Some work could also be done to find agreement between the differential amplifier and the laser as to the exact amount of time it takes the projectile to exit the rail after the cattle stunner has been fired. Since current densities are more concentrated on the corners and edges of the projectile, data needs to be gathered to determine the effect of changing projectile shape. Other materials should be tested and that could possibly lead to a pattern that can be matched against the periodic table of elements allowing for the classification of materials against the types of metals that could possibly be used for rail guns. The more information gathered on the topic, the sooner the rail gun can become the weapon of choice.

THIS PAGE INTENTIONALLY LEFT BLANK

LIST OF REFERENCES

1. Culpeper, W. C., *Rail Erosion and Projectile Diagnostics for an Electro-Magnetic Gun*, Master's Thesis, Naval Postgraduate School, Monterey, California, June 2002.

2. Adamy, M. T., *An Investigation of Sliding Electrical Contact in Rail Guns and the Development of Grooved-Rail Liquid-Metal Interfaces*, Master's Thesis, Naval Postgraduate School, Monterey, California, December 2001.

3. Beach, F. C., *Design and Construction of a One Meter Electromagnetic Railgu*n, Master's Thesis, Naval Postgraduate School, Monterey, California, June 1996.

4. Colombo, G. R., Otooni, M., Evangelisti, M. P., Colon, N., and Chu, E., *Applications of Coatings for Electromagnetic Gun Technology*, IEEE Transactions on Magnetics, Vol. 31, No. 1, 1995.

5. Electro-Magnetic Launch Workshop at the Institute for Advanced Technology, Austin, Texas, 7-9 November, 2001.

6. Feliciano, A. S., *The Design and Optimization of a Power Supply for a One-Meter Electromagnetic Railgun*, Master's Thesis, Naval Postgraduate School, Monterey, California, December 2001.

7. Gillich, D. J., *Design, Construction, and Operation of an Electromagnetic Railgun Test Bench*, Master's Thesis, Naval Postgraduate School, Monterey, California, June 2000.

8. Gurhan, Ozkan, *A Methodology to Measure Metal Erosion on Recovered Armatures*, Master's Thesis, Naval Postgraduate School, Monterey, California, December 2001.

9. Lockwood, M. R., *Design and Construction of an Expandable Series Augmented Electromagnetic Railgun*, Master's Thesis, Naval Postgraduate School, Monterey, California, June 1999.

10. Luke, I. T. and Stumborg, M. F., *The Operational Value of Long Range Land Attack EM Guns to Future Naval Force*s, IEEE Transactions on Magnetics, Vol. 37, No. 1, 2001.

11. Marshall, R. A., *Railgunnery: Where Have We Been? Where Are We Going?*, IEEE Transactions on Magnetics, Vol. 37, No. 1, 2001.

12. McNab, I. R., Fish, S., and Stefani, F., *Parameters for an Electromagnetic Naval Railgu*n, IEEE Transactions on Magnetics, Vol. 37, No. 1, 2001.

13. Nearing, J. C. and Huerta, M. A., *Skin and Heating Effects of Railgun Current*, IEEE Transactions on Magnetics, Vol. 25, No. 1, 1989.

14. Stefani, F., Levinson, S., Satapathy, S., and Parker, J., *Electrodynamic Transition in Solid Armature Railgun*s, IEEE Transactions on Magnetics, Vol. 37, No. 1, 2001.

INITIAL DISTRIBUTION LIST

1. Defense Technical Information Center
   Ft. Belvoir, Virginia

2. Dudley Knox Library
   Naval Postgraduate School
   Monterey, California

3. Professor William B. Maier II, Code PH/Mw
   Department of Physics
   Naval Postgraduate School
   Monterey, California

4. Professor Richard Harkins, Code PH
   Department of Physics
   Naval Postgraduate School
   Monterey, California

5. Lab Director Donald Snyder, Code PH
   Department of Physics
   Naval Postgraduate School
   Monterey, California

6. Engineering and Curriculum Officer, Code 34
   Naval Postgraduate School
   Monterey, California

7. Barbara M. Smith, Director
   Hampton University
   Computer Center
   Hampton, Virginia